

# REDDENING, ABSORPTION, AND DECLINE RATE CORRECTIONS FOR A COMPLETE SAMPLE OF TYPE Ia SUPERNOVAE LEADING TO A FULLY CORRECTED HUBBLE DIAGRAM TO $v < 30\,000 \text{ km s}^{-1}$

B. Reindl and G. A. Tammann

*Astronomisches Institut der Universität Basel,  
Venusstrasse 7, CH-4102 Binningen, Switzerland*

`G-A.Tammann@unibas.ch`

A. Sandage

*The Observatories of the Carnegie Institution of Washington,  
813 Santa Barbara Street, Pasadena, CA 91101*

and

A. Saha

*National Optical Astronomy Observatories,  
950 North Cherry Ave., Tucson, AZ 85726*

## ABSTRACT

Photometric ( $BVI$ ) and redshift data corrected for streaming motions are compiled for 111 “Branch normal”, four 1991T-like, seven 1991bg-like, and two unusual supernovae of type Ia. Color excesses  $E(B-V)_{\text{host}}$  of normal SNe Ia, due to the absorption of the host galaxy, are derived by three independent methods, giving excellent agreement leading to the intrinsic colors at maximum of  $(B-V)^{00} = -0.024 \pm 0.010$ , and  $(V-I)^{00} = -0.265 \pm 0.016$  if normalized to a common decline rate of  $\Delta m_{15} = 1.1$ .

The strong correlation between redshift absolute magnitudes (based on an arbitrary Hubble constant of  $H_0 = 60 \text{ km s}^{-1} \text{ Mpc}^{-1}$ ), corrected only for the extrinsic Galactic absorption, and the derived  $E(B-V)_{\text{host}}$  color excesses leads to the well determined, yet abnormal absorption-to-reddening ratios of  $\mathcal{R}_{BVI} = 3.65 \pm 0.16$ ,  $2.65 \pm 0.15$ , and  $1.35 \pm 0.21$ . Comparison with the canonical Galactic values of 4.1, 3.1, 1.8 forces the conclusion that the law of interstellar absorption

in the path length to the SN in the host galaxy is different from the local Galactic law, a result consistent with earlier conclusions by others.

Improved correlations of the fully corrected absolute magnitudes (on the same arbitrary Hubble constant zero point) with host galaxy morphological type, decline rate, and intrinsic color are derived. We recover the result that SNIa in E/S0 galaxies are  $\sim 0.3$  magnitudes fainter than in spirals for possible reasons discussed in the text. The new decline-rate corrections to absolute magnitudes are smaller than those by some authors for reasons explained in the text.

The four spectroscopically peculiar 1991T-type SNe are significantly overluminous as compared to Branch-normal SNe Ia. The overluminosity of the seven 1999aa-like SNe is less pronounced. The seven 1991bg-types in the sample constitute a separate class of SNe Ia, averaging in  $B$  two magnitudes fainter than the normal Ia.

New Hubble diagrams in  $B$ ,  $V$ , and  $I$  are derived out to  $\sim 30\,000 \text{ km s}^{-1}$  using the fully corrected magnitudes and velocities, corrected for streaming motions. Nine solutions for the intercept magnitudes in these diagrams show extreme stability at the 0.04 mag level using various subsamples of the data for both low and high extinctions in the sample, proving the validity of the corrections for host galaxy absorption. – The same precepts for fully correcting SN magnitudes we shall use for the luminosity recalibration of SNe Ia in the forthcoming final review of our HST Cepheid-SN experiment for the Hubble constant.

*Subject headings:* distance scale — galaxies: distances and redshifts — supernovae: general

## 1. INTRODUCTION

This is the third paper of a series whose purpose is to prepare for the projected final summary review of our 1991-2001 Hubble Space Telescope experiment to determine the Hubble constant by calibrating the absolute magnitude of type Ia supernovae. The method used in this observing program has been to measure Cepheid distances to the host galaxies by (1) correcting the raw Cepheid photometric data for reddening to determine the true distance moduli of the parent galaxies using an adopted Cepheid period-luminosity relation and (2) correcting the SNe data for their own intrinsic and extrinsic reddening and absorption values, plus all known second-parameter corrections for light-curve inhomogeneities.

The first two papers of this preparatory series concerned revisions in the Cepheid P-L relation and its lack of universality from galaxy to galaxy, showing significant differences

in the P-L slope and zero point between the Galaxy (Tammann et al. 2003) and the LMC (Sandage et al. 2004).

Following the emergence of SNe Ia as powerful standard candles (Kowal 1968), it became increasingly clear as the accuracy of the data became better that the dispersion in the SNe Ia absolute magnitude at maximum became smaller with each advance in the accuracy of the data (Sandage & Tammann 1982, 1993, 1997; Saha et al. 1997), and also with the application of corrections for light-curve inhomogeneities that had been found and subsequently systematically improved (Pskovskii 1967, 1971, 1984; Barbon et al. 1973; Phillips 1993; Sandage & Tammann 1995; Hamuy et al. 1995, 1996a,d; Tripp 1998; Phillips et al. 1999; Riess et al. 1999; Jha et al. 1999; Tripp & Branch 1999; Parodi et al. 2000; Tonry et al. 2003; also Sandage et al. 2001 for a review).

The purpose of this third paper of the series is to update the discussion by Parodi et al. (2000) on reddening, absorption, and second parameter corrections (decline rate, color, galaxy type) to the SNe Ia light curves, and to determine a revised Hubble diagram based on these corrections using the totality of the modern SNe Ia photometry available to date. The sample here consists of 124 supernovae compared with the sample of 35 SNe Ia used by Parodi et al..

The organization of the paper is this:

- (1) The photometric data for 124 SNe Ia are compiled in § 2 from the extensive literature, together with the types and recession velocities of their host galaxies (Table 1).
- (2) The *intrinsic* colors  $(B-V)_{\max}^{00}$ ,  $(B-V)_{35}^{00}$  (i.e. 35 days after  $B$  maximum), and  $(V-I)_{\max}^{00}$  are derived in § 3 from 34 normal SNe Ia which have occurred in E/S0 galaxies or in the outer regions of spiral galaxies and which are assumed – after correction for Galactic reddening – to suffer no reddening in their host galaxies.
- (3) After correction for Galactic reddening, the reddening of the normal SNe Ia due to the host galaxy is derived by three independent methods in § 4, leading to the intrinsic (unreddened) colors of each of the SNe. These corrected data are listed in Table 3a.
- (4) New absorption-to-reddening ratios for that part of the reddening due to the host galaxy are derived in § 5, leading to the absorption corrections to the observed SN apparent magnitudes (also corrected for the K-term effect due to redshift). The absorption-free magnitudes are also listed in Table 3a.
- (5) New dependencies of the fully corrected SN magnitudes on galaxy type, decline rate  $\Delta m_{15}$ , and intrinsic color are derived in § 6. Magnitudes  $m_{BVI}^{\text{corr}}$ , corrected for absorption and normalized to  $\Delta m_{15} = 1.1$  and  $(B-V)_{\max}^{00} = -0.024$  complete Table 3a.

(6) A discussion is made in § 7 of the photometric properties of the small group (15% of the total sample) of peculiar SNeIa, i.e. SNe-91T, SNe-99aa, SNe-91bg (named after their eponymous prototypes), and two singular objects (SN-2000cx, SN-1986G), with the conclusion that SNe-91T, including SNe-99aa, are brighter than normal SNeIa by 0.3 and 0.2 mag, respectively, even if normalized to  $\Delta m_{15} = 1.1$ , while SNe-91bg are underluminous in  $B$  by 2 mag.

(7) Hubble diagrams using  $m_{BVI}^{\text{corr}}$  are derived for various subsamples of normal SNeIa in § 8, together with the rms magnitude deviations for each of the subsamples used. The robustness of the solutions is emphasized.

(8) Twelve principal research points made in the paper are summarized in § 9.

The conventions used here are these: Colors  $(X - Y)_{\max}$  are always  $(X_{\max} - Y_{\max})$ .  $(X - Y)^0$  stands for colors corrected for Galactic reddening,  $(X - Y)^{00}$  for colors corrected for Galactic reddening *and* reddening in the host galaxy. Absolute magnitudes  $M_{BVI}$  and all listed distance moduli are calculated from the redshift using a flat universe with  $\Omega_{\text{matter}} = 0.3$ ,  $\Omega_{\Lambda} = 0.7$  with an arbitrarily assumed Hubble constant of  $H_0 = 60 \text{ km s}^{-1} \text{ Mpc}^{-1}$ . None of the conclusions as to magnitude corrections and trends of the second-parameter corrections depend on  $H_0$ , hence there is no loss of generality using any assumed value.

## 2. THE DATA

A list of 19 “local” ( $v_{220} < 2000 \text{ km s}^{-1}$ ) and 94 “nearby” ( $v_{\text{CMB}} \lesssim 30000 \text{ km s}^{-1}$ ) supernovae of Type Ia (SNeIa) after 1985 with available maximum magnitudes in  $B$  and  $V$ , and, if possible in  $I$ , is given in Table 1. The list aims to be complete as to published template-fitted maximum magnitudes in  $B$  and  $V$ , however the few nearby SNeIa with not so well observed lightcurves by Germany et al. (2004) are not considered. Eleven earlier SNeIa (9 “local” and 2 “nearby”) with useful photometry are added. Table 1 is subdivided into a) 111 spectroscopically “normal” SNeIa in the sense of Branch et al. (1993) including objects which are not spectroscopically confirmed but share the photometric properties of normal SNeIa (which is assumed here in first approximation also for the seven 1999aa-like objects); b) the four SNe-91T which are spectroscopically peculiar at early phases (Saha et al. 2001a; Li et al. 2001b); in addition included is the unique object SN 2000cx whose spectrum resembles SN 1991T at least near maximum phase (Li et al. 2001c; Candia et al. 2003); and c) the seven SNe-91bg objects which constitute a homogeneous sub-class with very fast decline rates ( $\Delta m_{15} \approx 1.9$ ), and which are quite red and underluminous at maximum. Also included here is SN 1986G; it has, however, a faster decline rate and much of its apparent redness is

probably due to absorption in the host galaxy.

Table 1 is organized as follows:

Col. 1: The name of the SN

Col. 2: The name of the host galaxy

Col. 3: The coded type of the host galaxy:  $E = -3$ ,  $E/S0 = -2$ ,  $S0 = -1$ ,  $S0/a = 0$ , the later types as in de Vaucouleurs et al. (1976). The galaxy types are taken from the same sources as the photometry, in some cases from van den Bergh et al. (2002, 2003).

Col. 4: The mean heliocentric radial velocity as given in the NASA Extragalactic Database (NED).

Col. 5: The radial velocity corrected for streaming motions. The nearer galaxies are corrected for a self-consistent Virgocentric infall model with a local infall vector of  $220 \text{ km s}^{-1}$  (Kraan-Korteweg 1986). The more distant galaxies are corrected for the CMB motion, where it is assumed that the co-moving volume extends to  $v_{220} = 3000 \text{ km s}^{-1}$ , justified by the kinematics of the “local bubble” that merges into the background field kinematics near  $3000 \text{ km s}^{-1}$  (Federspiel et al. 1994). Even if merging takes place as far out as  $6000 \text{ km s}^{-1}$  (Dale & Giovanelli 2000) it has no noticeable effect on the present results. If  $v_{220} < 3000 \text{ km s}^{-1}$ , the value of  $v_{220}$  is listed (denoted with v). All larger velocities are in the CMB frame. Virgo and Fornax cluster members are listed with the mean cluster velocity (denoted with V and F). Also two galaxies in the W-Cloud (NGC 4527, 4536) outside the Virgo cluster proper, are tentatively assigned the cluster velocity.

Col. 6-8: Observed  $B_{\max}$ ,  $V_{\max}$ , and  $I_{\max}$  magnitudes as compiled from Hamuy et al. (1996b,d), Riess et al. (1999), and Jha (2002). The latter has published the  $V$  and  $I$  magnitude at the epoch of the  $B$  maximum; they were transformed to  $V_{\max}$  and  $I_{\max}$  by interpolating Hamuy’s et al. (1996c) template light curves (their Table 10) with the appropriate decline rate  $\Delta m_{15}$ . Riess et al. (1999) have published only  $B$  and  $V$  maxima, their  $I$  photometry was reduced by Parodi et al. (2000) by the template method of Hamuy et al. (1996c) – which is also the procedure that provides the K-corrections for the effects of redshift on the photometry and which is the basis of all magnitudes in this paper. Where available the  $B_{\max}$  were taken from Altavilla et al. (2004) who have uniformly reduced the available data including various other sources. The corresponding  $V_{\max}$  are not published, but were kindly provided by Dr. G. Altavilla. Several additional sources are quoted in column 14.

Col. 9: The decline rate  $\Delta m_{15}$  taken from the same sources as the apparent maximum magnitudes. The slight dependence of  $\Delta m_{15}$  on the reddening (Phillips et al. 1999) is neglected.

Col. 10: The Galactic reddening following Schlegel et al. (1998)

Col. 11: The reddening  $E(B-V)_{\max}$  in the host galaxy as judged from the  $(B-V)^0$  color at maximum assuming intrinsic colors of  $(B-V)_{\max}^{00}$  as given in equation (1).

Col. 12: The reddening in the host galaxy at maximum as judged from the observed color

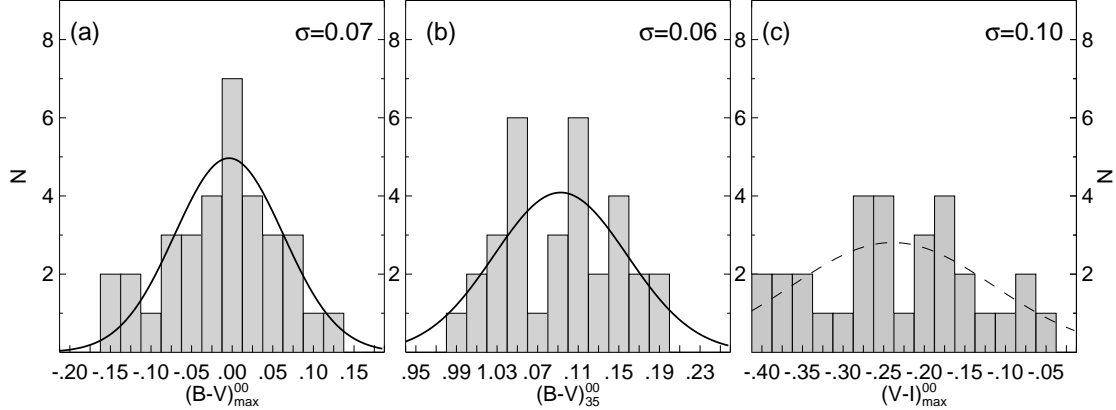


Fig. 1.— The true color distribution in  $(B-V)_{\max}^{00}$ ,  $(B-V)_{35}^{00}$ , and  $(V-I)_{\max}^{00}$  of SNe Ia with minimum reddening in their host galaxies from Table 2.

$(B-V)_{35}^{00}$  35 days past  $B$  maximum as explained in § 4.2.

Col. 13: The reddening in the host galaxy as judged from the  $(V-I)^0$  color at maximum assuming intrinsic colors  $(V-I)_{\max}^{00}$  as given in equation (3).

Col. 14: The source(s) of the photometry.

### 3. THE INTRINSIC COLOR OF SNe Ia

It is expected that SNe in early-type galaxies (S0 and earlier) as well as far outlying SNe in spiral galaxies suffer negligible reddening. In the case of SNe Ia in spiral galaxies we require that their distance  $r$  from the center of the host galaxy be larger than  $0.4r_{25}$ , where  $r_{25}$  is the isophote corresponding to 25 mag per arcsec<sup>2</sup> (cf. Parodi et al. 2000). A complete list of 34 such SNe Ia is given in Table 2 (omitting only the very red SN 1974G). Their colors  $(B-V)^0$ ,  $(B-V)_{35}^0$ , i.e. the color 35 days past  $B$  maximum from § 4.2 below, and  $(V-I)^0$ , all corrected for Galactic reddening (taken from column 10 of Table 1), are listed in Table 2. For the derivation of  $(V-I)^0$  it was assumed that  $E(V-I)_{\text{Gal}} = 1.3E(B-V)_{\text{Gal}}$ . The distribution of the colors is shown in Figure 1, their dependence on the decline rate  $\Delta m_{15}$  in Figure 2.

Since the SNe in Table 2 are assumed to suffer no reddening in their host galaxies, their Galactic absorption-corrected colors  $(X-Y)^0$  are equal to the colors  $(X-Y)^{00}$  corrected for Galactic *and* host galaxy reddening. The assumption of zero reddening is supported by several arguments. (a) If one assumes that the average error of  $B_{\max}$  and  $V_{\max}$  is 0.05, then

Table 2. SNe Ia with minimum reddening.

SN (1)	T (2)	$(B-V)_{\max}$ (3)	$E(B-V)_{\text{Gal}}$ (4)	$(B-V)_{\max}^0$ (5)	$(B-V)_{35}^0$ (6)	$(V-I)_{\max}^0$ (7)	$\Delta m_{15}$ (8)
(a) SNe in early-type galaxies							
1990af	-1	0.07	0.035	0.035	1.048	...	1.59
1992J	-2	0.12	0.057	0.063	1.107	-0.194	1.69
1992ae	-3	0.08	0.036	0.044	1.159	...	1.30
1992au	-3	0.04	0.017	0.023	1.050	-0.402	1.69
1992bk	-3	-0.07	0.015	-0.085	1.047	-0.090	1.67
1992bo	-2	0.02	0.027	-0.007	1.031	-0.145	1.69
1992bp	-2	0.00	0.069	-0.069	1.103	-0.240	1.52
1992br	-3	0.07	0.026	0.044	1.043	...	1.69
1993O	-2	-0.07	0.053	-0.123	1.082	-0.199	1.26
1993ac	-3	0.17	0.163	0.007	1.092	-0.082	1.25
1993ae	-3	-0.10	0.038	-0.138	1.013	-0.179	1.47
1993ag	-2	0.18	0.112	0.068	1.160	-0.246	1.30
1993ah	-1	-0.04	0.020	-0.060	1.142	-0.316	1.45
1994D	-1	-0.08	0.022	-0.102	1.028	-0.199	1.31
1994M	-3	0.05	0.023	0.027	1.184	-0.130	1.45
1994Q	-1	0.08	0.017	0.063	1.130	-0.292	0.90
1996X	-3	0.05	0.069	-0.019	1.073	-0.270	1.32
1997E	-1	0.14	0.124	0.016	1.103	-0.171	1.39
1998dx	-3	-0.03	0.041	-0.071	...	-0.173	1.55
1999gh	-3	0.19	0.058	0.132	1.123	-0.055	1.69
2000B	-3	0.17	0.068	0.102	1.117	-0.258	1.46
2000dk	-3	0.07	0.070	0.000	1.001	-0.271	1.57
(b) Outlying SNe in spirals							
1972E	Am	0.00	0.056	-0.056	1.048	-0.383	1.05
1990N	3	0.02	0.026	-0.006	1.195	-0.254	1.05
1990O	1	0.08	0.093	-0.013	1.117	-0.411	0.94
1990T	1	-0.08	0.053	-0.133	1.172	-0.079	1.13
1991S	3	0.03	0.026	0.004	1.154	-0.274	1.00
1991ag	3	0.11	0.062	0.048	1.109	-0.351	0.87
1992A	0	0.01	0.018	-0.008	1.043	-0.273	1.47
1992bc	2	-0.12	0.022	-0.142	0.990	-0.339	0.90
1992bl	0	-0.03	0.011	-0.041	1.036	-0.234	1.56
1995D	0	0.04	0.058	-0.018	1.146	-0.375	1.03
1998V	3	0.17	0.196	-0.026	1.088	-0.165	1.06
1998eg	5	0.12	0.123	-0.003	...	-0.150	1.15
mean [ $N = 34, 32, 31$ ]:				-0.013	1.092	-0.232	
random error of mean:				$\pm 0.012$	$\pm 0.010$	$\pm 0.018$	
$\sigma$ :				0.07	0.06	0.10	

the observed scatter of  $\sigma_{B-V} = 0.07$  mag in Table 2 is fully explained by these errors. In that case the distribution of  $(B-V)_{\max}^0$  in Figure 1a must be Gaussian, which is statistically acceptable in spite of the four very blue SNe Ia with  $(B-V)_{\max}^0 < -0.12$ . (b) As Figure 1 shows, the color distribution of the SNe Ia in Table 2 is skewed bluewards, if anything, while any noticeable reddening would skew the distribution towards red colors. (c) The colors

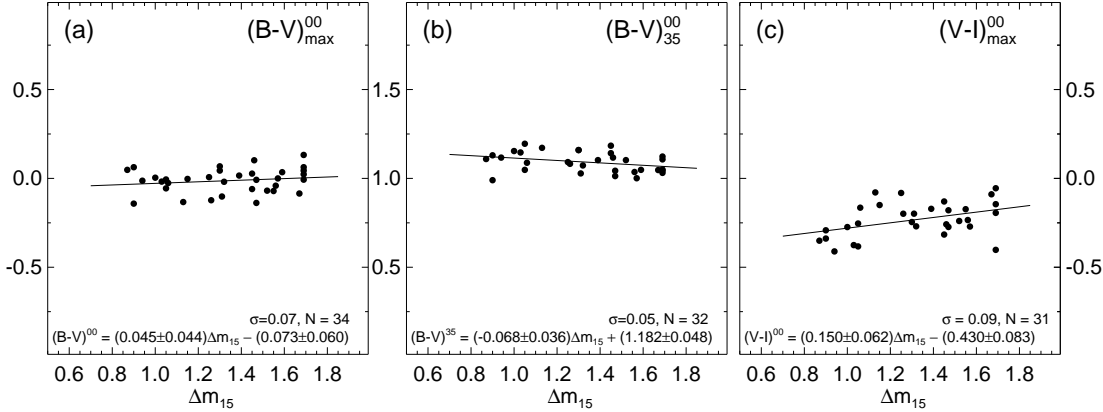


Fig. 2.— The dependence of the colors  $(B-V)_{\max}^{00}$ ,  $(B-V)_{35}^{00}$ , and  $(V-I)_{\max}^{00}$  of the SNe Ia in Table 2 on the decline rate  $\Delta m_{15}$ .

$(B-V)_{\max}^{00}$  and  $(V-I)_{\max}^{00}$  of the SNe Ia in Table 2 are *uncorrelated* (in fact insignificantly anti-correlated); in case of absorption in the host galaxies both values would be redder than average. (d) If the spread in color in Figure 1a was due to absorption, the absolute magnitudes  $M_B$  would correlate with the color  $(B-V)_{\max}^0$  from column 5 with a slope of  $\mathcal{R}_B = 3.65$ , whereas an insignificant slope of  $0.137 \pm 0.904$  is observed.

The least squares solutions of the data in Figure 2 are

$$(B-V)_{\max}^{00} = (0.045 \pm 0.044)\Delta m_{15} - (0.073 \pm 0.060), \sigma = 0.07, N = 34 \quad (1)$$

$$(B-V)_{35}^{00} = (-0.068 \pm 0.036)\Delta m_{15} + (1.182 \pm 0.048), \sigma = 0.05, N = 32 \quad (2)$$

$$(V-I)_{\max}^{00} = (0.150 \pm 0.062)\Delta m_{15} - (0.430 \pm 0.083), \sigma = 0.09, N = 31. \quad (3)$$

The dependence of  $(B-V)_{\max}^{00}$  on  $\Delta m_{15}$  in equation (1) is weaker than suggested by Phillips et al. (1999), Nobili et al. (2003), and Altavilla et al. (2004). In fact the dependence is only marginally significant. Yet it is adopted here at face value. – The similarity of SNe Ia spectra at  $t_B = 35^d$  and the similar slopes of the color curves at this late phase have led Lira (1995), Riess et al. (1996), Phillips et al. (1999), and Altavilla et al. (2004) to assume that  $(B-V)_{35}^{00}$  is independent of  $\Delta m_{15}$ . However, equation (2) shows this color to become *bluer* with increasing  $\Delta m_{15}$  at a significance of  $2\sigma$ . – The  $(V-I)_{\max}^{00}$  colors exhibit in equation (3) a clear dependence on  $\Delta m_{15}$ , becoming *redder* with increasing decline rate.

The mean intrinsic colors of normal SNe Ia, normalized to  $\Delta m_{15} = 1.1$ , become from equations (1–3)

$$(B-V)_{\max}^{00} = -0.024 \pm 0.010, (B-V)_{35}^{00} = 1.107 \pm 0.009, \text{ and } (V-I)_{\max}^{00} = -0.265 \pm 0.016. \quad (4)$$

Having argued that SNe Ia in Table 2 are essentially reddening-free, it is nevertheless clear that their reddening is not exactly zero. Their true colors must therefore be slightly bluer than expressed in equation (4). We will return to this point in § 9 where it is stressed that any rest reddening is inconsequential for the use of SNe Ia as standard candles as long as they are reduced to some *uniform* color.

#### 4. THE REDDENING OF SNe Ia IN THEIR HOST GALAXIES

The reddening  $E(B-V)_{\text{host}}$  of SNe Ia at maximum phase due to selective absorption in the host galaxy is determined in three different ways.

##### 4.1. The Reddening in the Host Galaxy from $(B-V)_{\text{max}}^{00}$

The reddening in the host galaxy is given by

$$E(B-V)_{\text{max}} = B_{\text{max}} - V_{\text{max}} - E(B-V)_{\text{Gal}} - (B-V)_{\text{max}}^{00}. \quad (5)$$

$E(B-V)_{\text{max}}$  follows for all SNe Ia in Table 1a and tentatively for the peculiar SNe Ia in Table 1b by inserting the apparent magnitudes and the Galactic reddening from columns 6, 7, and 10 in Table 1a,b and by taking the intrinsic color from equation (1). The resulting  $E(B-V)_{\text{max}}$  are given in column 11 of Table 1a & b.

##### 4.2. The Reddening in the Host Galaxy from the Tail Colors $(B-V)_{35}^{00}$

Color excesses  $E(B-V)_{35}$  at phase  $t_B = 35$  days were kindly provided by S. Jha for 59 SNe Ia in Table 1a. He has based them on an adopted intrinsic tail color of  $(B-V)_{35}^{00} = 1.055$  for all SNe Ia. Additional tail color excesses were published by Phillips et al. (1999) and Altavilla et al. (2004). They are in a slightly different system as those by Jha. In a first step the Altavilla excesses were transformed into Jha's system by the regression

$$\Delta E(B-V)_{\text{Alta-Jha}} = (0.048 \pm 0.032)E(B-V)_{\text{Alta}} + (0.020 \pm 0.006), \sigma = 0.03, N = 38. \quad (6)$$

In a second step the Phillips excesses were transformed by comparison with the joint set from Jha and Altavilla by means of

$$\Delta E(B-V)_{\text{Phil-Jha}} = (0.084 \pm 0.025)E(B-V)_{\text{Phil}} + (0.018 \pm 0.009), \sigma = 0.06, N = 62. \quad (7)$$

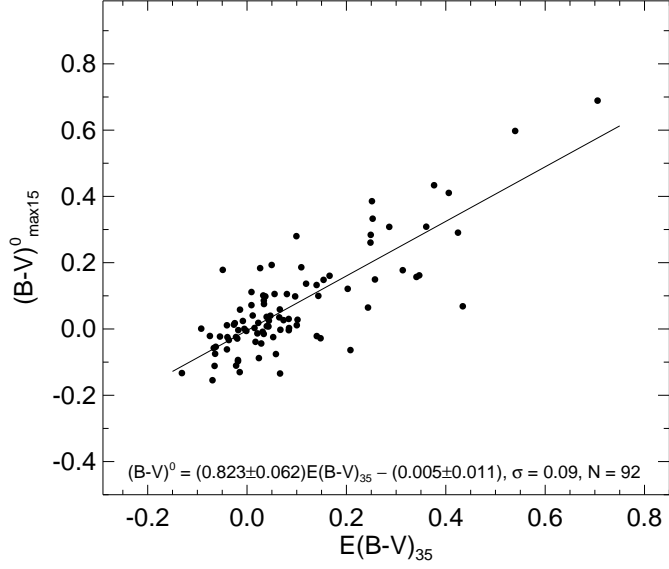


Fig. 3.— The relation of the colors  $(B-V)_{\max 15}^0$  versus the reddening values  $E(B-V)_{35}$  which are derived from a *red* SN phase.

The homogenized excesses  $E(B-V)_{35}$  of SNeIa with more than one determination were averaged. If one adds to these values Jha's adopted intrinsic color of  $(B-V)_{35}^{00} = 1.055$ , one recovers the "observed" tail colors  $(B-V)_{35}^0$ , not listed, for 105 of the SNeIa.

New color excesses  $E(B-V)_{35}$  are now determined by making allowance for the  $\Delta m_{15}$  dependence of the intrinsic color  $(B-V)_{35}^{00}$ . This is achieved by subtracting  $(B-V)_{35}^{00}$  as given in equation (2) from the "observed" colors  $(B-V)_{35}^0$ .

The adopted tail excesses  $E(B-V)_{35}$  apply to the quite red phase at  $t_B = 35^d$ . They cannot directly be applied to the (blue) SN colors at maximum, because  $E(B-V)$  must depend on color due to bandwidth effects. In fact, if one plots the colors  $(B-V)_{\max 15}^0$  (corrected for Galactic reddening and reduced to  $\Delta m_{15} = 1.1$  with equation (1)) against the adopted values of  $E(B-V)_{35}$  one obtains the following linear regression (Figure 3).

$$(B-V)_{\max 15}^0 = (0.823 \pm 0.062)E(B-V)_{35} - (0.005 \pm 0.011), \sigma = 0.09, N = 92 \quad (8)$$

Since the *intrinsic* color  $(B-V)^{00}$  at maximum must not be a function of reddening it follows from equation (8) that

$$E(B-V)_{\max 35} = (0.823 \pm 0.062)E(B-V)_{35}. \quad (9)$$

The resulting values  $E(B-V)_{\max 35}$  are listed in Table 1a, column 12. The excesses from

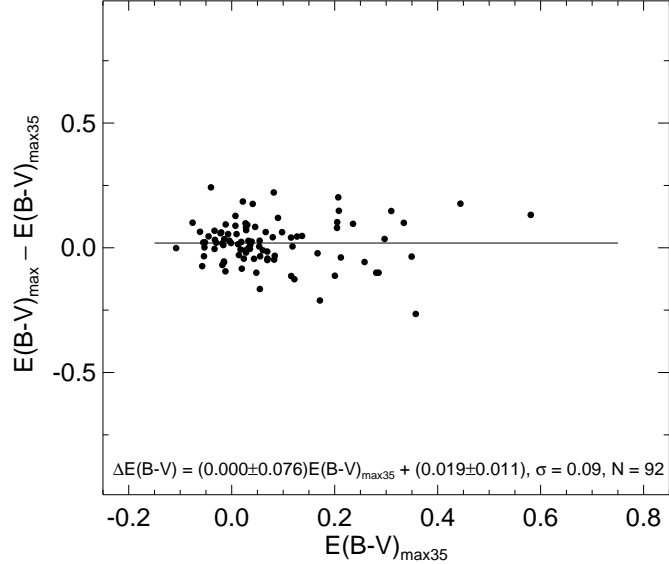


Fig. 4.— Comparison of the color excesses  $E(B - V)_{\max}$  from colors at maximum and  $E(B - V)_{\max35}$  from tail colors at  $t_B = 35^d$ .

equations (5 & 9) are compared in Figure 4. The agreement is satisfactory with no systematic differences.

The excesses  $E(B - V)_{\max35}$  for four peculiar SNe Ia in Table 1b are given in parentheses. They are smaller on average than their excesses from  $(B - V)_{\max}$ , suggesting that they are redder at  $t_B = 35^d$  than normal SNe Ia (see also § 7.1). The excesses  $E(B - V)_{\max35}$  of the SN 1991bg-like SNe in Table 1c have not been used, but they are consistent with the assumption that these SNe in early-type galaxies are almost reddening-free.

#### 4.3. The Reddening in the Host Galaxy from $(V - I)_{\max}^{00}$

A third possibility to determine the reddening  $E(B - V)$  in the host galaxy is provided by the magnitudes  $V_{\max}$  and  $I_{\max}$  in Table 1a & b, columns 7 & 8. We note

$$E(V - I) = V_{\max} - I_{\max} - 1.3E(B - V)_{\text{Gal}} - (V - I)_{\max}^{00}, \quad (10)$$

where  $E(V - I) = 1.3E(B - V)$  is adopted for the Galactic reddening. If one inserts the intrinsic colors from equation (3), with the  $\Delta m_{15}$ -values appropriate for each SNe Ia, into equation (10) one obtains  $E(V - I)$ .

Since  $E(B - V)$  is required, not  $E(V - I)$ , the latter must be converted into the former.

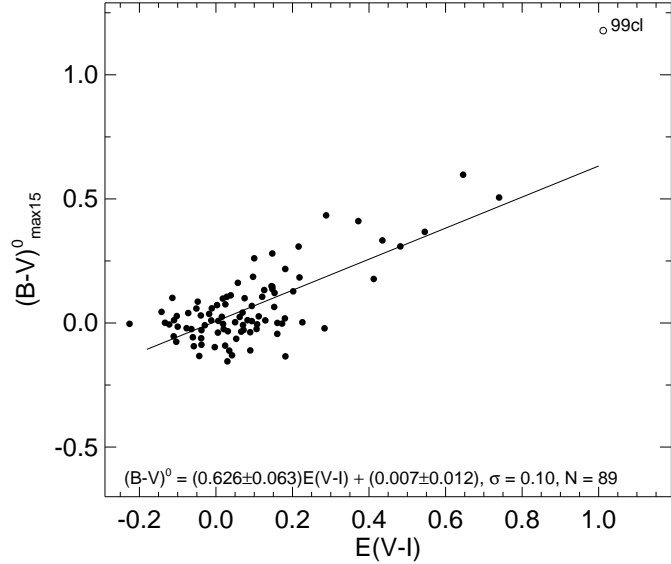


Fig. 5.— The correlation of the color  $(B-V)_{\text{max15}}^0$  and  $E(V-I)$ . SN 1999cl is not taken into account.

This is done by means of Figure 5, where  $(B-V)_{\text{max15}}^0$  (as in Figure 3) is plotted against  $E(V-I)$ . From the equation at the bottom of Figure 5 follows

$$E(B-V)_{\text{max}}^{V-I} = (0.626 \pm 0.063)E(V-I). \quad (11)$$

The color excesses  $E(B-V)_{\text{max}}^{V-I}$ , listed in column 13 of Table 1, are compared with the mean of the excesses  $E(B-V)_{\text{max}}$  and  $E(B-V)_{\text{max35}}$  in Figure 6. Again the agreement is satisfactory.

#### 4.4. The Adopted Reddening in the Host Galaxies

In view of the consistency of the color excesses  $E(B-V)_{\text{max}}$ ,  $E(B-V)_{\text{max35}}$ , and  $E(B-V)_{\text{max}}^{V-I}$  they are averaged with equal weights. The means are adopted as the best estimates of the reddening in the host galaxy,  $E(B-V)_{\text{host}}$ . The values of  $E(B-V)_{\text{host}}$  are listed in Table 3, column 2. The ensuing colors  $(B-V)_{\text{max}}^{00}$ , fully corrected for Galactic and host galaxy reddening, are in column 3.

Table 3 is organized as follows:

Col. 1: The name of the SN.

Col. 2: The adopted reddening  $E(B-V)_{\text{host}}$  in the host galaxy being the mean of columns

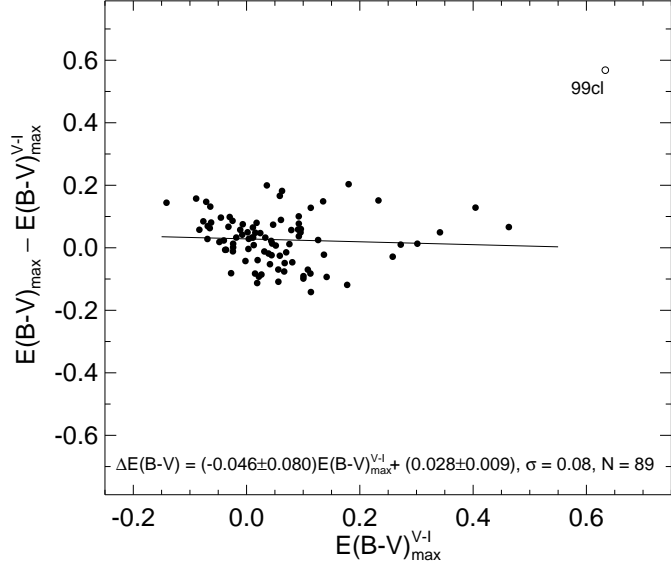


Fig. 6.— The difference  $E(B-V)_{\max}$  minus  $E(B-V)_{\max}^{V-I}$  plotted against  $E(B-V)_{\max}^{V-I}$ .  $E(B-V)_{\max}$  is here the mean of  $E(B-V)_{\max}$  and  $E(B-V)_{\max}^{35}$ .

11-13 of Table 1.

Col. 3&4: The intrinsic colors  $(B-V)_{\max}^{00}$  and  $(V-I)_{\max}^{00}$  corrected for Galactic reddening and reddening in the host galaxy.

Col. 5-7: The apparent magnitudes  $m_{BVI}^{00}$  at maximum, corrected for absorption in the Galaxy and in the host galaxy.

Col. 8-10: The absorption-corrected apparent magnitudes  $m_{BVI}^{\text{corr}}$  reduced to a standard decline rate of  $\Delta m_{15} = 1.1$  and  $(B-V)_{\max}^{00} = -0.024$  by the precepts developed in § 6.4.

Col. 11: The photometric absorption-free distance modulus  $(m - M)_{\text{lum}}^{00}$  from  $m_V^{\text{corr}}$  in column 9 and the mean luminosity  $M_V^{\text{corr}}$  in equation (28). The latter assumes  $H_0 = 60$ .

In order to free the  $(V-I)^0$  colors from the host galaxy reddening the relation between  $E(V-I)_{\text{host}}$  and  $E(B-V)_{\text{host}}$  is needed. It is obtained from Figure 7, where  $(V-I)^0$  is plotted versus  $E(B-V)_{\text{host}}$ . The figure yields (slightly rounded)

$$E(V-I)_{\text{host}} = (1.32 \pm 0.07)E(B-V)_{\text{host}}, \quad (12)$$

which we adopt. The conversion factor is consistent with equation (11), but here  $E(B-V)_{\text{host}}$  has high weight being the mean of three determinations. The rms dispersion of  $E(B-V)_{\text{host}}$ , if based on the three determinations, is 0.043 mag.

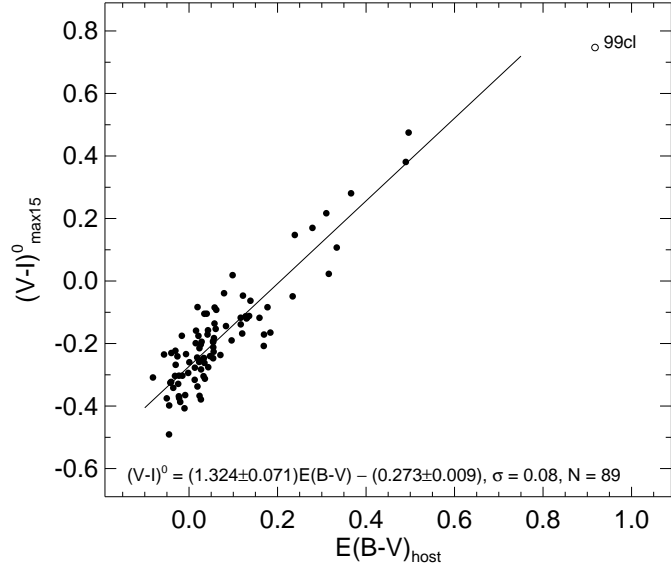


Fig. 7.— The colors  $(V - I)_{\text{max15}}^0$ , corrected for Galactic reddening, versus the adopted reddening  $E(B - V)_{\text{host}}$  in the host galaxy.

#### 4.5. Test of the K-Correction

The template-fitting of the SN light curves by the method of Hamuy et al. (1996c) is applied in a way as to compensate the K-correction, i.e. the effect of the redshifts  $z$  on the magnitudes and colors, in a single step. To verify the success of the method we plot the adopted colors  $(B - V)_{\text{max15}}^{00}$  and  $(V - I)_{\text{max15}}^{00}$ , normalized to  $\Delta m_{15} = 1.1$ , against  $\log cz$  in Figure 8. Any dependence is hardly significant and is neglected in the following.

### 5. THE ABSORPTION-CORRECTED MAGNITUDES OF SNe Ia

#### 5.1. The Galactic Absorption

The Galactic reddenings of Schlegel et al. (1998) are converted into absorption values  $A_B$ ,  $A_V$ , and  $A_I$  by means of conventional absorption-reddening ratios of  $\mathcal{R}_B = 4.1$ ,  $\mathcal{R}_V = 3.1$ , and  $\mathcal{R}_I = 1.8$  (hence  $E(V - I) = 1.3E(B - V)$  as used in § 3). The resulting absorption values are subtracted from the observed SN magnitudes to obtain  $B^0$ ,  $V^0$ , and  $I^0$  at maximum.

Conventional values of  $\mathcal{R}$  have been adopted because the available range of  $E(B - V)_{\text{Gal}}$  is too small to derive meaningful Galactic  $\mathcal{R}$  values from the SNe Ia themselves.

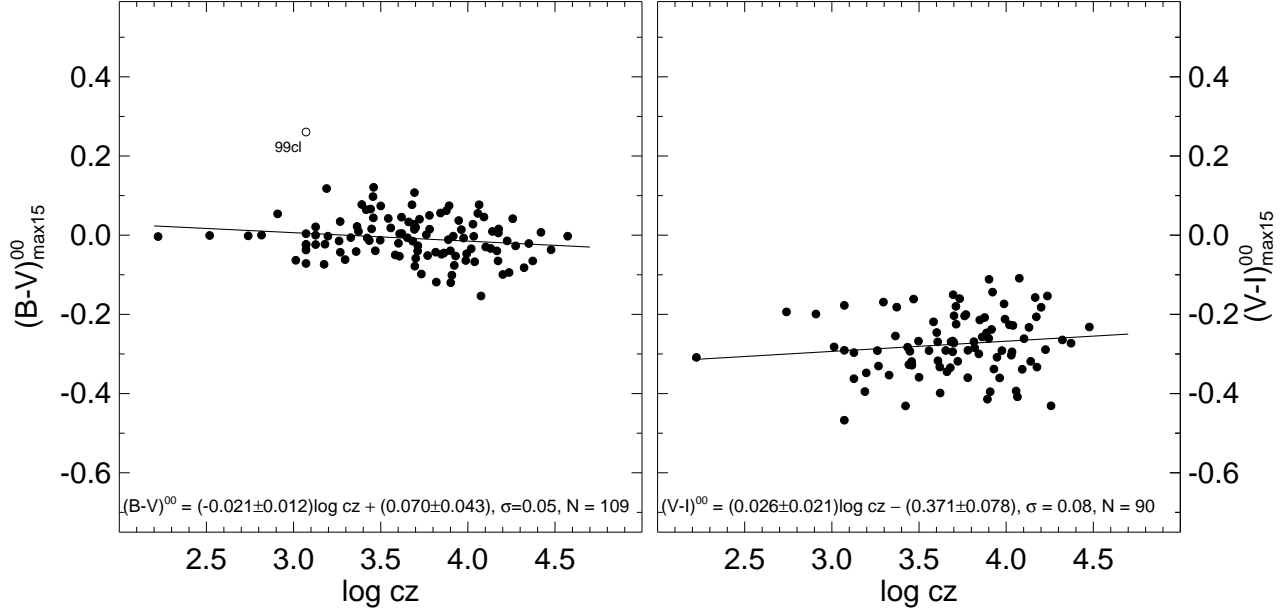


Fig. 8.— A test of the adopted K-corrections. The colors  $(B-V)_{\max 15}^{00}$  and  $(V-I)_{\max 15}^{00}$ , normalized to  $\Delta m_{15} = 1.1$ , show only a negligible correlation.

## 5.2. The Absorption in the Host Galaxy

Previous attempts to correct SN magnitudes for absorption in the host galaxies have frequently assumed conventional (Galactic) values of  $\mathcal{R}_{BVI}$ , although Branch & Tammann (1992, and references therein) have argued for significantly smaller values. More recent determinations are (quoted  $\mathcal{R}_V$  values are transformed here to  $\mathcal{R}_B$  by  $\mathcal{R}_B \equiv \mathcal{R}_V + 1$ )  $\mathcal{R}_B = 3.55 \pm 0.30$  (Riess et al. 1996), 2.09 (Tripp 1998),  $3.5 \pm 0.4$  (Phillips et al. 1999), 2.8 (Krisciunas et al. 2000),  $3.88 \pm 0.15$  (Wang et al. 2003), 3.5 (Altavilla et al. 2004). The present large sample of SNe Ia is well suited for an independent determination of the average value of  $\mathcal{R}_{BVI}$  of extragalactic SNe Ia.

For this purpose the absolute magnitudes  $M_{BVI}^0$ , based on  $H_0 = 60$  and corrected only for Galactic absorption, are plotted against the values of the host galaxy reddening  $E(B-V)_{\text{host}}$  as listed in column 13 of Table 1 (Figure 9).

The SN sample used here is called in the following the “fiducial” sample. It contains the 62 (58) SNe Ia in Table 1a with  $B$ ,  $V$  (and  $I$ ) magnitudes and with  $3000 < v_{\text{CMB}} < 20\,000 \text{ km s}^{-1}$ . It excludes SN 1996ai which suffers excessive absorption in its host galaxy (see Table 1a). It also excludes five SNe Ia, which deviate by more than  $2\sigma_M$ . The apparently normal SN 1999ej is too faint for unknown reasons by  $3\sigma_M$ . SN 1992ag is very red at  $t_{35}$ ,

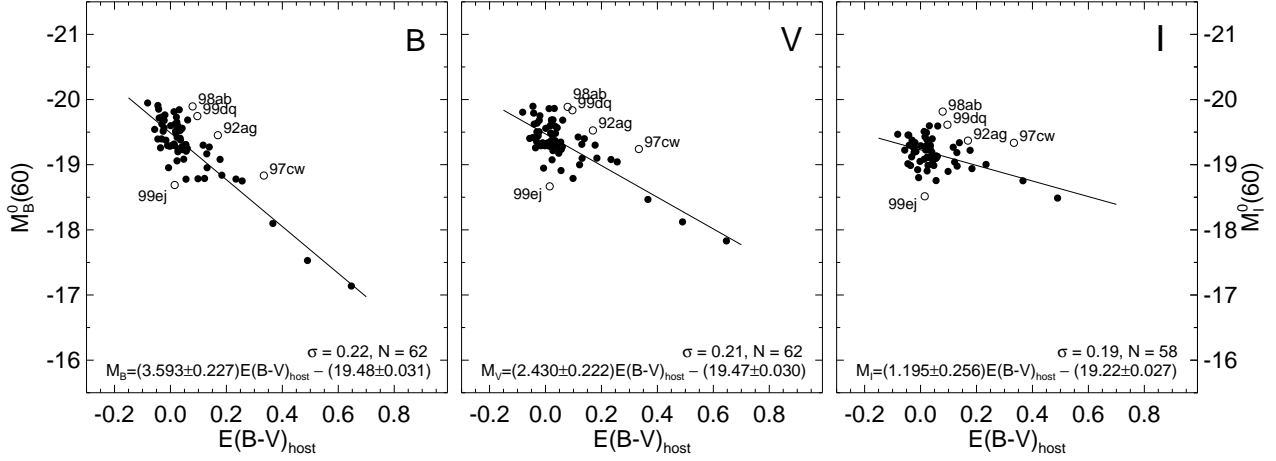


Fig. 9.— The dependence of the absolute magnitudes  $M_{BVI}^0(60)$  on the host galaxy reddening  $E(B-V)_{\text{host}}$  for SNe Ia with  $3000 < v_{\text{CMB}} < 20000 \text{ km s}^{-1}$ . The  $M_{BVI}^0$  magnitudes are only corrected for Galactic absorption. Five SNe Ia shown here as open symbols are not used for the solution (see text).

causing its tail excess  $E(B-V)_{\text{max35}}$  to be large, which in turn makes  $(B-V)_{\text{max}}^{00}$  exceptionally blue and the absolute magnitude very bright (cf. Table 1a and 3). It is believed that either its color  $(B-V)_{35}^0$  is in error or its light curve is peculiar. If the color excess was based only on the color at maximum its absolute magnitude would become normal. The overly bright SN 1997cw is suspicious not so much because its photometry begins only 16 days after  $B$  maximum, but because it was classified as SNe-91T (Berlind et al. 1997), which is now revised to SNe-91T/99aa (Li et al. 2001b). Also the very luminous SN 1998ab and 1999dq are of type SNe-99aa (Li et al. 2001b). The properties of this new class of SNe Ia and their overluminosity are taken up again in § 7.1.

Four other less overluminous SNe-99aa, designated with a dagger † in Table 1a, are kept in the sample of normal SNe Ia. The reason is that they can be isolated only from pre-maximum spectroscopy, which is lacking for many objects in Table 1a. Thus a few of the “normal” SNe Ia may actually belong to the elusive class of SNe-99aa without having as extreme luminosities like SN 1997cw, 1998ab, and 1999dq.

As shown by the equations in Figure 9 the resulting values of  $\mathcal{R}_{BVI}$  are about 3.6, 2.4, and 1.2. However, these values are still open to criticism. As will be shown below SNe Ia in E/S0 have lower intrinsic luminosities *and* less extinction than average. Therefore there is some dependence of  $M_{BVI}^0$  on  $E(B-V)$  which cannot be attributed to absorption, but which is due to the intrinsic underluminosity of SNe Ia in early-type galaxies. This type-dependent effect can be compensated by the decline rate  $\Delta m_{15}$  in § 6.2. The interplay of  $\mathcal{R}$  and  $\Delta m_{15}$

requires therefore a simultaneous solution which is given in equation (15) below. From this the improved values of  $\mathcal{R}_{BVI}$  become

$$\mathcal{R}_B = 3.65 \pm 0.16, \quad \mathcal{R}_V = 2.65 \pm 0.15, \quad \mathcal{R}_I = 1.35 \pm 0.21. \quad (13)$$

The  $\mathcal{R}$  values here are in addition adjusted to fulfill the condition  $\mathcal{R}_B - \mathcal{R}_V = 1$ . They are quite close to the provisional values in Figure 9. It is also satisfactory that they agree quite well with those by other authors cited above.

If one assumes that the highly reddened SN 1996ai is a normal SNe Ia with average luminosity and that its peculiar motion is  $\lesssim 200 \text{ km s}^{-1}$ , one finds  $\mathcal{R}_B = 3.0 \pm 0.4$  from this single object.

The solutions in Table 4 for  $\mathcal{R}_V$  and  $\mathcal{R}_I$  imply a ratio  $E(V-I)/E(B-V) = \mathcal{R}_V - \mathcal{R}_I = 1.21 \pm 0.26$ , which may be compared with  $1.32 \pm 0.07$  from equation (12). The small error of the latter value is due to the fact that its determination is independent of any assumed value of  $\mathcal{R}$ , which is notoriously difficult to determine. It is noted that the adopted value of 1.30 is the same as the conventional Galactic value of 1.3.

The values of  $E(B-V)_{\text{host}}$  (Table 3, column 2) were multiplied with the  $\mathcal{R}_{BVI}$  values in equation (13) to be subtracted from the apparent magnitudes  $B$ ,  $V$ , and  $I$  (Table 1, columns 6-8), after they are corrected for the conventional Galactic absorption. The resulting fully corrected apparent magnitudes  $m_{B \text{ max}}^{00}$ ,  $m_{V \text{ max}}^{00}$ , and  $m_{I \text{ max}}^{00}$  are tabulated in columns 5-7 of Table 3.

## 6. THE DEPENDENCE OF SN LUMINOSITIES ON OTHER PARAMETERS

### 6.1. The Dependence of SN Luminosities on Galaxy Type

If one plots the absolute magnitudes  $M_V^{00}$  as introduced in § 5, but now also corrected for absorption in the host galaxy and *without* the  $\Delta m_{15}$  correction, against the Hubble type of the host galaxy, a clear correlation emerges between SN luminosity and the Hubble type as first shown by Hamuy et al. (1996a, 2000), the SNe Ia in early-type galaxies being fainter by  $\sim 0.3$  mag than in late spirals (Figure 10). The obvious conclusion is that young populations produce brighter SNe Ia.

Yes, but why? The most secure conclusion from the data, which are beyond doubt (Hamuy et al. 1995; Saha et al. 1997, 1999; Parodi et al. 2000; Sandage et al. 2001, Fig. 6), is that different channels of SNe Ia production exist between most SNe Ia in E/S0 galaxies compared with most SNe Ia in spirals.

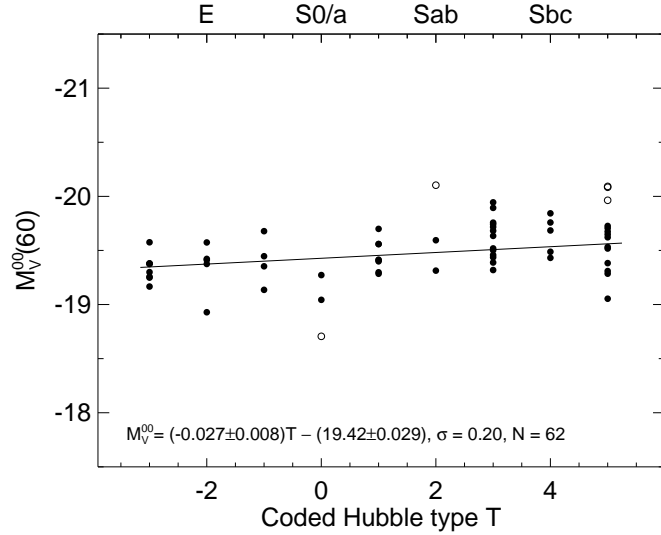


Fig. 10.— The correlation between the absolute magnitudes  $M_V^{00}(60)$ , fully corrected for absorption, and the coded Hubble type of the host galaxy.

Both channels are fed by old, highly evolved stars near one solar mass that are in close binaries. By one of two processes (mass transfer from a normal star to a white dwarf, or mergers of two white dwarfs due to orbital energy loss caused by gravitational radiation nudging one or both stars over the Chandrasekhar limit), catastrophic collapse eventually occurs, but with different gestation times. Hence, the delay times differ for progenitor formation to explosion, according to the process. The consequence is that the star formation rates of the initial progenitors differ between E/S0 galaxies and spirals (E/S0 with a single burst of star formation early on; spirals with a more continuous star formation rate). Hence, the average delay times differ between E/S0 and spirals (L. Greggio, private communication), making a difference in the Fe production rate, hence a chemical composition difference. This expected chemical composition difference apparently affects the absolute magnitude at maximum in the SN explosion, as suggested by Hamuy et al. (2000).

## 6.2. The Dependence of SN Luminosity on Light Curve Parameters

Since also the decline rate is a function of the Hubble type, one expects a correlation between the luminosity and the decline rate as well. This Pskovskii effect was first quantified by the decline rate parameter  $\Delta m_{15}$  by Phillips (1993). The corresponding correlation of the form

$$M_{BVI15}^{00} = M_{BVI}^{00} - \alpha_{BVI}(\Delta m_{15} - 1.1) \quad (14)$$

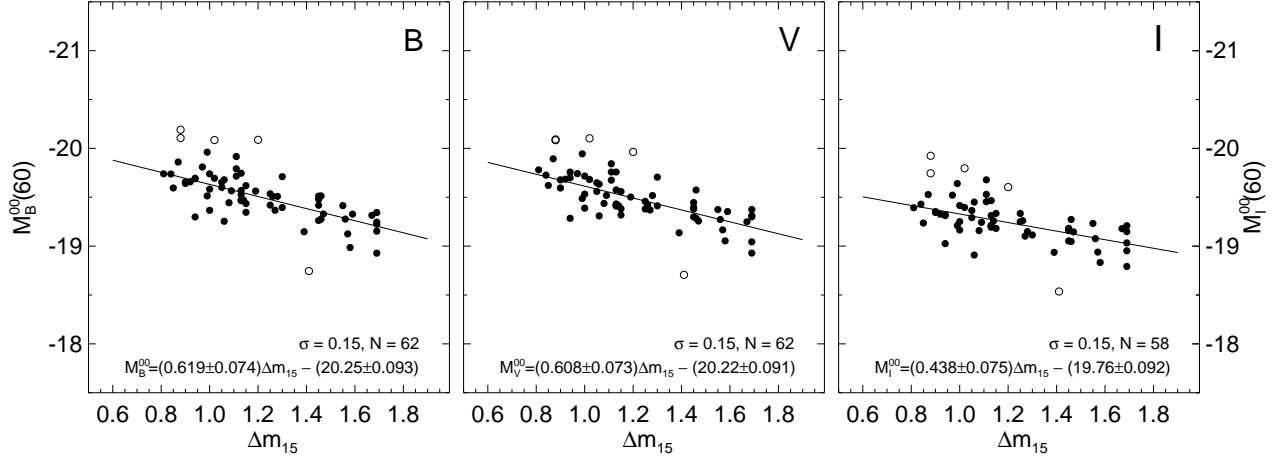


Fig. 11.— The dependence of the absolute magnitudes  $M_{BVI}^{00}(60)$  on the decline rate  $\Delta m_{15}$ . The SNeIa with open symbols have not been used for the solution. They are identified in Figure 9 and discussed in § 5.2.

is in fact even tighter than the one in Figure 10; it is shown in Figure 11. The normalization to  $\Delta m_{15} = 1.1$  corresponds roughly to the median value of normal SNeIa. The magnitudes  $M_{BVI}^{00}$  are corrected for Galactic and internal absorption described in § 5.

Since  $\alpha$  and  $\mathcal{R}$  and hence  $M^{00}$  are not quite independent, as discussed in § 5.2, these quantities must be simultaneously solved for. The corresponding regression with two independent variables takes the form of

$$M_{BVI}^0 = \alpha_{BVI}(\Delta m_{15} - 1.1) + \mathcal{R}_{BVI}E(B-V)_{\text{host}} + M_{BVI15}^{00}, \quad (15)$$

where the constant term,  $M_{BVI15}^{00}$ , is the mean absolute magnitude of SNeIa, corrected for Galactic and host galaxy absorption and reduced to  $\Delta m_{15} = 1.1$ . Least-squares solutions for the same fiducial SN sample as used for Figure 9 give the values of  $\alpha_{BVI}$ ,  $\mathcal{R}_{BVI}$ , and  $M_{BVI15}^{00}$  as shown in Table 4.

The values of  $\alpha_{BVI}$  in Table 4 will be adopted in the following. The dependence of  $M_{BVI}^{00} = M_{BVI}^0 - \mathcal{R}_{BVI}E(B-V)_{\text{host}}$  on  $\Delta m_{15}$  is illustrated in Figure 11, where  $\alpha_{BVI}$  appears as the slope of the correlation.

The values of  $\mathcal{R}_{BVI}$  in Table 4 differ slightly from the values in equation (13), which we have adopted as the final ones, because the latter comply with the additional conditions that  $\mathcal{R}_B - \mathcal{R}_V = 1$  and  $\mathcal{R}_V - \mathcal{R}_I = 1.3$  from equation (12).

In equation (1) it was shown that the color  $(B-V)_{\text{max}}^{00}$  is only marginally dependent on

Table 4. The coefficient  $\alpha$  of the decline rate, the absorption-to-reddening ratio  $\mathcal{R}$ , and the absorption-corrected mean absolute magnitude of normal SNe Ia with  $\Delta m_{15} = 1.1$ .

	<i>B</i>	<i>V</i>	<i>I</i>
$\alpha$	$0.619 \pm 0.076$	$0.608 \pm 0.074$	$0.438 \pm 0.076$
$\mathcal{R}$	$3.75 \pm 0.16$	$2.59 \pm 0.15$	$1.38 \pm 0.21$
$M_{15}^{00}(60)$	$-19.57 \pm 0.02$	$-19.55 \pm 0.02$	$-19.28 \pm 0.02$
$\sigma_M$	0.15	0.15	0.15
$N$	62	62	58

$\Delta m_{15}$ . This is vindicated here by the  $\alpha$ 's in Table 4. They yield for the relation

$$(B-V)_{\max}^{00} = \beta \Delta m_{15} + \text{const} \quad (16)$$

an insignificant value of  $\beta = \alpha_B - \alpha_V = 0.011 \pm 0.106$ . The corresponding coefficient for the  $(V-I)_{\max}^{00}$  colors becomes  $\alpha_V - \alpha_I = 0.170 \pm 0.106$ , which is consistent with  $0.150 \pm 0.062$  from equation (3).

It becomes clear from the above that any change of  $\beta$  affects necessarily the coefficients  $\alpha$ , because an excess  $\Delta\beta$  causes a change of the color excess of

$$\Delta E(B-V)_{\max} \propto -\Delta\beta \Delta m_{15}. \quad (17)$$

This affects the absorption-corrected magnitudes  $M_B^{00}$ , taken as an example, by

$$\Delta M_B^{00} \propto \mathcal{R}_B \Delta\beta \Delta m_{15}. \quad (18)$$

Hence, if the *intrinsic* dependence of  $M_B$  on  $\Delta m_{15}$  is  $\Delta M_B^{00} \propto \alpha \Delta m_{15}$ , one observes instead

$$\Delta M_B^{00} \propto (\alpha_B + \mathcal{R}_B \Delta\beta) \Delta m_{15}. \quad (19)$$

The analogue holds for the color excesses  $E(B-V)_{35}$  derived from tail colors  $(B-V)_{35}^0$ . If the true colors vary like  $\Delta(B-V)_{35}^0 \propto \gamma \Delta m_{15}$ , any deviation  $\Delta\gamma$  from  $\gamma$  leads to a variation of the color excess of

$$\Delta E(B-V)_{35} \propto -\Delta\gamma \Delta m_{15}, \quad (20)$$

such that  $\Delta E(B-V)_{\text{host}}$ , being the mean of  $\Delta E(B-V)_{\max}$  and  $\Delta E(B-V)_{35}$ , varies like

$$\Delta E(B-V)_{\text{host}} = -\frac{1}{2}(\Delta\beta + \Delta\gamma) \Delta m_{15}, \quad \text{and} \quad (21)$$

$$\Delta M_B^{00} \propto [\alpha_B + \frac{1}{2}\mathcal{R}_B(\Delta\beta + \Delta\gamma)] \Delta m_{15} = (\alpha_B + \Delta\alpha) \Delta m_{15}. \quad (22)$$

We have adopted, besides  $\mathcal{R}_B = 3.65$ ,  $\beta = 0.045$  (equation 1),  $\gamma = -0.068$  (equation 2) as the intrinsic values. Yet some authors have adopted other values of  $\mathcal{R}$ ,  $\beta$  and  $\gamma$  which necessarily reflect on the observed value of  $\alpha$ . For instance Phillips et al. (1999) have chosen  $\Delta\beta = 0.069$ ,  $\Delta\gamma = 0.068$ , and  $\mathcal{R}_B = 4.16$ . If one subtracts the resulting  $\Delta\alpha = 0.285$  from their proposed value  $\alpha' = 0.786 \pm 0.398$  one obtaines  $\alpha_B = 0.501 \pm 0.398$ . Altavilla et al. (2004) have taken  $\Delta\beta = 0.045$ ,  $\Delta\gamma = +0.068$ , and  $\mathcal{R}_B = 3.5$ ; this leads to  $\Delta\alpha = 0.198$  which, subtracted from their preferred value  $\alpha' = 1.061 \pm 0.154$ , yields  $\alpha_B = 0.863 \pm 0.154$ . These two determinations of  $\alpha_B$  embrace the adopted value of  $\alpha_B = 0.612 \pm 0.073$  in Table 5 within statistics. – If we had set the coefficient  $\beta = 0.045 \pm 0.044$  in equation (1) equal to 0, as Parodi et al. (2000) did, the present fiducial sample would give  $\alpha_B = 0.532 \pm 0.083$  which is the same as their value within the errors.

The correlation of type-Ia SN luminosity and light curve shape has a considerably history. First suggested by Pskovskii (1967, 1971, 1984) it was taken up by Barbon et al. (1973). Phillips (1993) used first the decline rate  $\Delta m_{15}$  to parametrize the correlation, however he had to depend on inaccurate Tully-Fisher and surface brightness fluctuation distances, which resulted in an overestimate of the slope  $\alpha_B$  by a factor of  $\sim 4.5$ . The steep slope was the reason why Sandage & Tammann (1995) questioned the correlation altogether. If Phillips had been correct in the steepness of the Pskovskii effect, implying a luminosity variation of 2.5 mag in  $B$  over the full range of  $\Delta m_{15}$ , the use of SNe Ia as standard candles would have been substantially compromised. Only when sufficient relative velocity distances became available the determination of the slope  $\alpha$  began to converge (Hamuy et al. 1996b; Phillips et al. 1999; Parodi et al. 2000; Sandage et al. 2001; Altavilla et al. 2004). The remaining differences are now explained by the sensitivity of  $\alpha$  on the adopted relation between color and  $\Delta m_{15}$  (equations 1–3).

From the above it is clear that a positive/negative excess of the coefficient  $\beta$  in equation (1) propagates into  $E(B-V)_{\text{host}}$  and into the absorption values such that the magnitudes  $M_{\text{max}}^{00}$  (or  $m_{\text{max}}^{00}$ ) are too faint/bright by  $\mathcal{R}\Delta\beta\Delta m_{15}$ . Yet it is to be noted that the magnitudes  $M_{\text{max}15}^{00}$ , normalized to  $\Delta m_{15} = 1.1$ , are not affected by this error, because they are corrected by an additional term  $\Delta\alpha\Delta m_{15} = \mathcal{R}\Delta\beta\Delta m_{15}$  of opposite sign. The error compensation is only exact if  $E(B-V)_{\text{host}}$  is determined from the intrinsic colors given in equation (1). In the present case also the intrinsic colors from equations (2 & 3) are used to determine  $E(B-V)_{\text{host}}$ , but the three determinations agree so well that it is sufficient here to show that any effect of an incorrect value of  $\beta$  on  $M_{\text{max}15}^{00}$  is compensated by the adopted value of  $\alpha$  in Table 4.

Perlmutter et al. (1997) have introduced the “stretch factor”,  $s$ , instead of  $\Delta m_{15}$  to characterize the light curve shape. The two parameters  $s$  and  $\Delta m_{15}$  show a tight correlation

(Jha 2002; Altavilla et al. 2004); they are interchangeable for all practical purposes.

An alternative method to allow for the correlation between luminosity and light curve shape and to determine at the same time the total absorption  $A_V$  was introduced by Riess et al. (1996, 1998, see also Jha 2002; Wang et al. 2003; Tonry et al. 2003). Their various forms of “Multi-color Light Curve Shape” (MLCS) fitting are difficult to apply and offer no obvious advantages.

### 6.3. The Dependence of the SN Luminosity on the Color

Following a proposal by Tripp (1998) and Parodi et al. (2000) we test the question whether SN luminosity depends on the color  $(B-V)_{\max}^{00}$  and/or  $(V-I)_{\max}^{00}$  in Figure 12. Dependencies at the  $\gtrsim 2\sigma$  level seem to exist of  $M_{B\max 15}^{00}$  and  $M_{I\max 15}^{00}$  on  $(B-V)_{\max}^{00}$  and of  $M_{I\max 15}^{00}$  on  $(V-I)_{\max}^{00}$  (see equations at the panel bottoms of Figure 12). The correlations should be considered, however, with some reservations because the range of about  $\pm 0.15$  mag in either color is only about two times the estimated observational error of a single color determination (about  $\pm 0.07$  mag).

In the following the correlation of SN luminosity on  $(B-V)_{\max}^{00}$  is taken at face value.  $(B-V)$  colors are preferred over  $(V-I)$  colors because the latter are not available for all SNeIa of the fiducial sample. The allowance for the color dependence does not shift the mean luminosity of SNeIa, but brings a marginal decrease of the luminosity dispersion, at least in  $I$ . In any case the allowance for color can bring no harm.

### 6.4. SN Magnitudes Corrected for $\Delta m_{15}$ and Color

From the discussion in § 6.2 and 6.3 follows that minimum scatter of the absolute magnitude  $M_{BVI}^{00}$  can be achieved by correcting for the decline rate  $\Delta m_{15}$  and color  $(B-V)_{\max}^{00}$ . The corresponding ansatz

$$M_{BVI}^{00} = a(\Delta m_{15} - 1.1) + b[(B-V) + 0.024] + c \quad (23)$$

leads with the fiducial sample of 62 SNeIa to the coefficients  $a$ ,  $b$ , and  $c$  in Table 5.

If one subtracts the first two terms of equation (23) from the fully absorption-corrected magnitudes  $m_{BVI}^{00}$  in columns 5-7 Table 3 one obtains the magnitudes  $m_{BVI}^{\text{corr}}$  (columns 8-10) which are in addition reduced to  $\Delta m_{15} = 1.1$  and a corresponding color of  $(B-V)_{\max}^{00} = -0.024$ . The distribution functions of the resulting absolute magnitudes  $M_{BVI}^{\text{corr}}$  of the fiducial

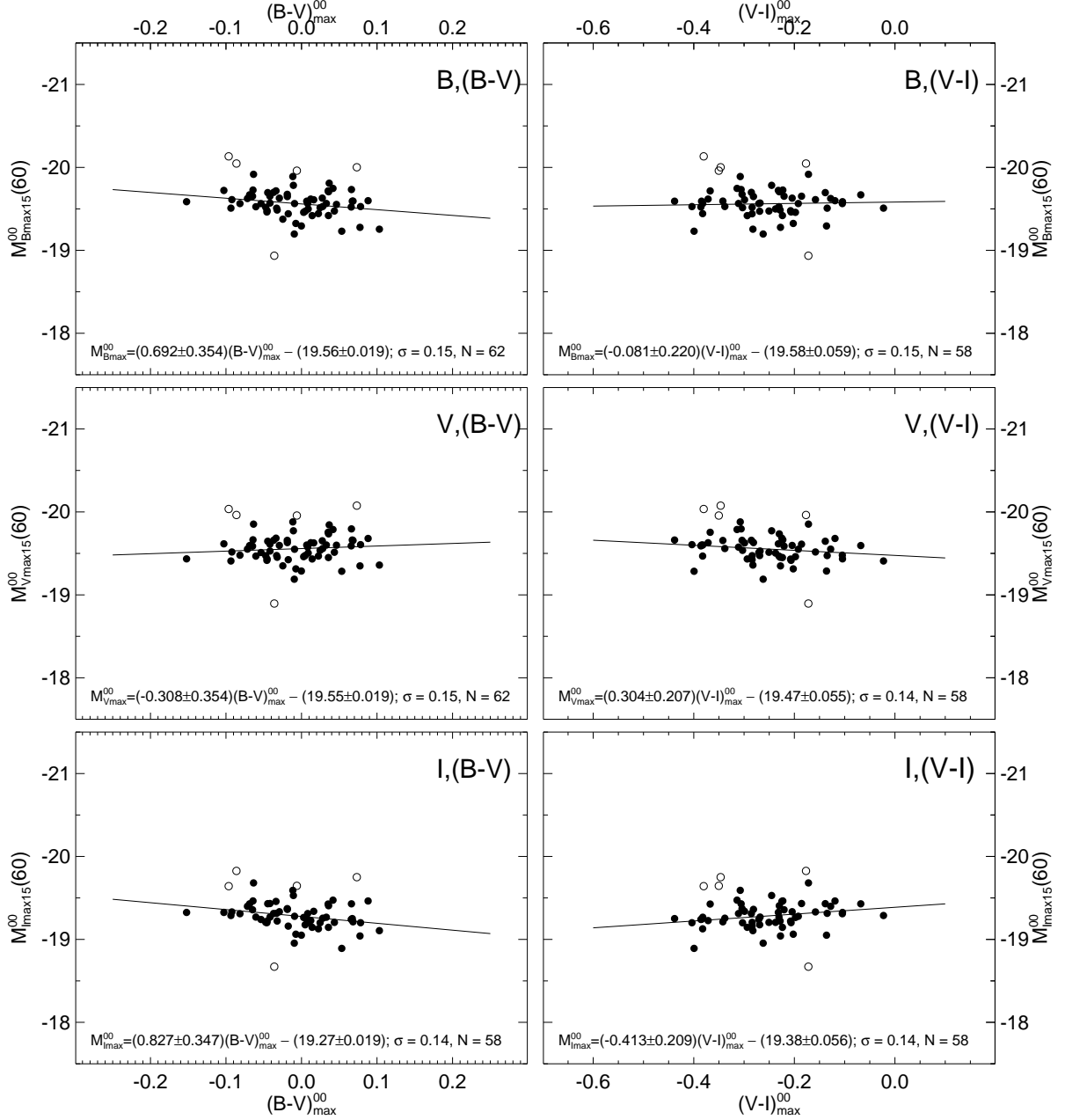


Fig. 12.— The dependence of the absolute magnitudes  $M_{BVI}^{00}$  on the color  $(B-V)_{\max}^{00}$  and  $(V-I)_{\max}^{00}$ . The SNeIa with open symbols have not been used for the solution. They are identified in Figure 9.

sample – always on the basis of  $H_0 = 60$  – are shown in Figure 13. They are well fitted by Gaussians after five SNeIa, discussed in § 5.2, are excluded.

Table 5. The coefficients in equation (23).

	<i>a</i>	<i>b</i>	<i>c</i>	$\sigma$	<i>N</i>
with $(B-V)_{\max}^{00}$					
$M_B, (B-V)$ :	$0.612 \pm 0.073$	$0.692 \pm 0.357$	$-19.57 \pm 0.02$	0.15	62
$M_V, (B-V)$ :	$0.612 \pm 0.073$	$-0.308 \pm 0.357$	$-19.55 \pm 0.02$	0.15	62
$M_I, (B-V)$ :	$0.439 \pm 0.072$	$0.827 \pm 0.350$	$-19.29 \pm 0.02$	0.14	58

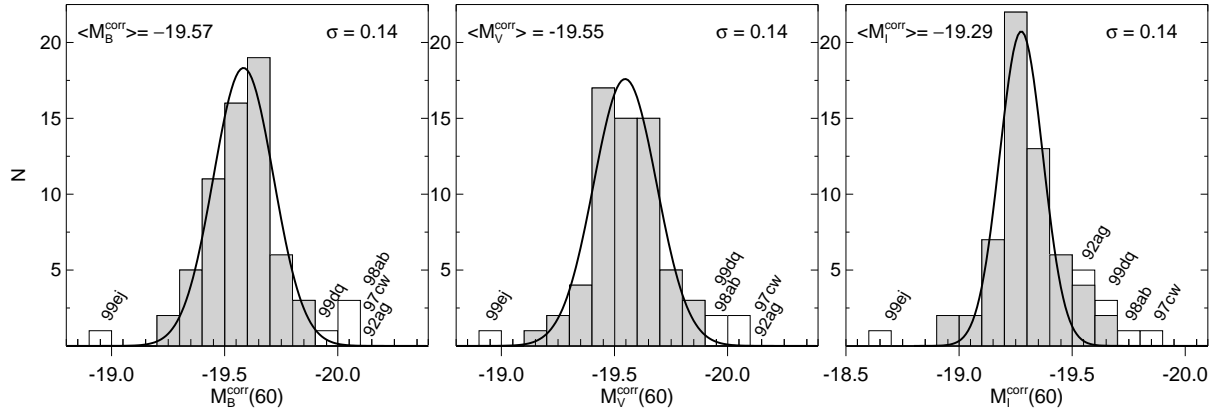


Fig. 13.— The distribution in absolute magnitude  $M_{BVI}^{\text{corr}}$  of the 62 (58) SNe Ia with  $3000 < v < 20000 \text{ km s}^{-1}$ . Additional five SNe Ia as in Figure 9 are identified; they are not used for the solution.

## 7. PHOTOMETRIC PROPERTIES OF PECULIAR SNe Ia (SNe-91T AND SNe-91bg AND TWO OTHERS)

### 7.1. SNe-91T and SNe-99aa

SNe-91T, with SN 1991T as the prototype and long suspected to be overluminous, are spectroscopically well defined (e.g. Li et al. 2001b, and references therein). The observed and derived photometric properties of the known quartet are listed in Table 1b and 3b, respectively. They are characterized by quite slow decline rates  $\Delta m_{15}$ . Their intrinsic color  $(B-V)_{\max}^{00}$ , being unknown, was *assumed* to be given by equation (1) like that of normal SNe Ia. If one derives color excesses  $E(B-V)_{\text{host}}$  and absorption values on this basis, one finds the mean photometric parameters given in Table 6. The fact that the resulting mean value of  $\langle (V-I)_{\max}^{\text{corr}} \rangle = -0.29$  is similar to normal SNe Ia shows that the present assumption

Table 6. Mean photometric parameters of SNe-91T, SNe-99aa, and SN 2000cx (not reduced to a common  $\Delta m_{15}$  or color).

		$\Delta m_{15}$	$(B-V)_{\max}^{00}$	$(V-I)_{\max}^{00}$	$M_{B \max}^{00}$	$M_{V \max}^{00}$	$M_{I \max}^{00}$
		(1)	(2)	(3)	(4)	(5)	(6)
SNe-91T	mean	0.95	–0.03 <sup>a</sup>	–0.29	–20.01 <sup>b</sup>	–19.98 <sup>b</sup>	–19.63 <sup>b</sup>
		±.03		±.06	±.08	±.08	±.12
	N	4	4	3	4	4	3
-----							
SNe-99aa	mean	0.92	–0.01 <sup>c</sup>	–0.34	–19.88	–19.87	–19.53
		±.03	±.01	±.05	0.10	±.10	±.10
	N	7	7	7	7	7	7
-----							
SN 2000cx		0.97	–0.03 <sup>a</sup>	–0.61	–20.39	–20.36	–19.75
	or		0.09 <sup>d</sup>	–0.46	–19.96	–20.05	–19.59

<sup>a</sup> $(B-V)_{\max}^{00}$  assumed to be –0.030 from equation (1)

<sup>b</sup>For SN 1991T the Cepheid distance of  $(m - M)^0 = 30.74$  was adopted (Saha et al. 2001a)

<sup>c</sup>On the assumption that  $(B-V)_{\max}^{00}$  and  $(B-V)_{35}^{00}$  are given by equation (1 & 2) for normal SNe Ia

<sup>d</sup>Allowing only for Galactic absorption and assuming zero reddening in the S0 host galaxy

on  $(B-V)_{\max}^{00}$  leads at least to consistent results. Their absolute magnitudes  $M_{BVI}^{00}$ , as given in Table 6, turn out to be brighter than normal SNe Ia (equation 28 below) by  $\Delta M_B = -0.40 \pm 0.08$  on average with remarkably small scatter. Even if one reduces their luminosity to  $\Delta m_{15} = 1.1$  (equation 14) they remain overluminous by  $-0.32 \pm 0.08$ . This conclusion could only be avoided by postulating that SNe-91T were very blue at maximum, i.e.  $(B-V)_{\max}^{00} \approx -0.11$ . This is, however, not supported by interstellar absorption lines which give  $(B-V)_{\max}^{00} = -0.04$  to  $+0.06$  for SN 1991T (Filippenko et al. 1992) and  $(B-V)_{\max}^{00} = -0.03$  for SN 1997br (Li et al. 1999).

SNe-91T are rare events. Four representatives out of a total of 124 corresponds to a relative frequency of about 3%. A few unrecognized SNe-91T may have to be added, but on the other hand their presumed overluminosity enhances their discovery chance, which is further enhanced by their slow decline rates. Hence a rate of roughly 3% seems realistic.

Li et al. (2001b) have noted in the pre-maximum spectra of some SNe Ia features typical for normal SNe Ia and others typical for SNe-91T (see also Garavini et al. 2004). At maximum

and later they have normal spectra. The prototype is SN 1999aa; the class is here designated as SNe-99aa. Seven SNeIa in Table 1 were classified as SNe-99aa by Li et al. (2001b); they are marked with a dagger. If one determines their host galaxy extinction on the assumption that they have  $(B-V)$  colors at maximum and at  $t_B = 35^d$  like normal SNeIa, their average color  $(V-I)_{\max}^{00}$  becomes roughly the same as for normal SNeIa as seen in Table 6. Since SNe-99aa are spectroscopically a milder form of SNe-91T one expects that their luminosity lies between the latter and normal SNeIa. This expectation is born out in Table 6. SNe-99aa are brighter by only  $\Delta M_B = -0.30 \pm 0.10$  than normal SNeIa, which is further reduced to  $-0.19 \pm 0.10$  if normalized to  $\Delta m_{15} = 1.1$ .

If overluminosity and strikingly slow decline rates ( $\Delta m_{15} < 1.02$ ) are typical for SNe-99aa, it is noted that Table 1a contains 13 additional possible candidates. At least three of them are normal SNeIa (SN 1997bp, Anupama 1997 and references therein; SN 1998ef, Li et al. 2001b; and SN 2000E, Valentini et al. 2003), leaving 10 candidates at most. If they are added to the 7 known cases, the total of known or unrecognized SNe-99aa in Table 1 is  $\leq 14\%$ , i.e. less than estimated by Li et al. (2001b). Their true frequency in a volume-limited sample may be even lower considering that their suggested overluminosity and their slow decline rates favor their discovery.

## 7.2. SNe-91bg

Seven SNeIa in Table 1b (excluding SN 1986G) are of type SNe-91bg with SN 1991bg as the prototype. They are characterized by peculiar spectra (Mazzali et al. 1997, and references therein), very red color, low luminosity and unparalleledly fast decline rates  $\Delta m_{15}$ . Their rate of occurrence seems high in early-type galaxies. This offers a handle on their intrinsic properties, because the four known SNe-91bg in early-type galaxies may be assumed to have minimum reddening. Since the remaining three SNe-91bg in spirals are not significantly redder [ $\Delta(B-V)_{\max}^{00} = 0.66 \pm 0.09$  versus  $0.59 \pm 0.08$ ] we assume that the internal reddening of this class can be neglected. Minimal reddening is also independently confirmed for SN 1999bg in the spiral NGC 2841 from late-phase multi-color photometry (Garnavich et al. 2004). The ensuing mean photometric parameters are compiled in Table 7.

The SNe-91bg emerge – besides for their spectral peculiarities – as a separate class of SNe with quite narrowly confined photometric properties. Their decline rate varies little about  $\Delta m_{15} = 1.91$ , while no normal SNIa is known with  $\Delta m_{15} \gtrsim 1.7$ . Their extremely red intrinsic colors have only moderate scatter. In fact their  $(V-I)_{\max}^{00}$  shows less scatter than normal SNeIa. Their absolute magnitudes show somewhat more variation than normal SNeIa, but they are all strikingly underluminous by  $\Delta M_B = 2.11 \pm 0.16$ ,  $\Delta M_V = 1.48 \pm 0.14$ ,

Table 7. Mean photometric parameters of SNe-91bg.

	$\Delta m_{15}$ (1)	$(B-V)_{\max}^{00}$ (2)	$(V-I)_{\max}^{00}$ (3)	$M_{B_{\max}}^{00}$ (4)	$M_{V_{\max}}^{00}$ (5)	$M_{I_{\max}}^{00}$ (6)
mean	1.91	0.62	0.23	−17.46 <sup>a</sup>	−18.07 <sup>a</sup>	−18.30 <sup>a</sup>
	±.02	±.06	±.03	±.16	±.14	±.11
$\sigma$	0.04	0.15	0.09	0.42	0.37	0.30
N	7	7	7	7	7	7
-----						
86G	1.69 or	0.00 <sup>b</sup> 0.43 <sup>c</sup>	...	−19.16 <sup>d</sup> −17.58 <sup>d</sup>	−19.16 <sup>d</sup> −18.01 <sup>d</sup>	...

<sup>a</sup>Adopting for SN 1999by the Cepheid distance of  $(m - M)^0 = 30.74$  (Macri et al. 2001)

<sup>b</sup> $(B-V)_{\max}^{00}$  assumed to be 0.00 as for all normal SNe Ia with  $\Delta m_{15} = 1.69$  (see equation 1)

<sup>c</sup> $(B-V)_{35}^{00}$  assumed to be 1.067 as for normal SNe Ia with  $\Delta m_{15} = 1.69$  (see equation 2)

<sup>d</sup>Adopting for the parent galaxy NGC 5128 (Cen A)  $(m - M)^0 = 27.80$  (Thim et al. 2003)

and  $\Delta M_I = 0.93 \pm 0.11$  on average. The underluminosity may be somewhat reduced if we have underestimated the host galaxy absorption, but we deem values as large as  $A_{B_{\text{host}}} \approx 0.3$  (and correspondingly less in  $V$  and  $I$ ) as unlikely. Models of two SN-91bg (SN 1991bg and SN 1999by) were elaborated by Mazzali et al. (1997) and by Höflich et al. (2002).

The frequency per unit volume of SNe-91bg can roughly be estimated by noting that the seven known cases all lie within  $5000 \text{ km s}^{-1}$ , and that Table 1a contains 47 SNe Ia within this distance limit. Of these, 45 have  $\Delta m_{15} < 1.7$  and the remaining two (SN 1981D and 1984A) are normal SNe Ia on the basis of their colors. Hence seven cases out of a total of 54 correspond to a frequency of 13%, or somewhat more because their fast decline rates impair their discovery probability (see also Li et al. 2001a). Since they occur preferentially in early-type galaxies, it is suggested that they stem from an older population (Howell 2001).

### 7.3. Two Additional Peculiar SNe Ia (SN 2000cx AND SN 1986G)

Only two SNe Ia in Table 1 are neither normal nor belong to the SNe-91T (including SNe-99aa) and SNe-91bg classes.

### 7.3.1. SN 2000cx

The spectrum of SN 2000cx resembles SNe-91T at early phases, but its light curve is highly unusual, in fact unique (Li et al. 2001c; Candia et al. 2003). The observed photometric parameters are given in Table 1b. The intrinsic photometric properties at maximum are calculated here for two different assumptions. a) The SN has  $(B-V)_{\max}^{00} = -0.01$  like normal SNe Ia, or b) The SN suffers zero reddening in its S0 host galaxy. The ensuing colors and luminosities are shown in Table 6. In either case SN 2000cx may be with  $M_{B\max}^{00} \lesssim -20.0$  one of the brightest SN in the entire sample. Fisher et al. (1999) have argued that such high luminosities, although still depending on the exact value of  $H_0$ , require one Chandrasekhar mass of pure  $^{56}\text{Ni}$  which cannot be provided by a single White Dwarf. They proposed therefore a model with two merging White Dwarfs. SN 2000cx may be a prime candidate for this process.

### 7.3.2. SN 1986G

The spectrum of SN 1986G is similar to SNe-91bg, but less extreme (Cristiani et al. 1992, and references therein). Its photometric observables are in Table 1c. They show that SN 1986G was observed to be even redder than SNe-91bg, but to have a clearly slower decline rate. Much of its redness is certainly due to its position in the dust lane of NGC 5128 (Cen A).

The intrinsic color and luminosity are calculated here for two different assumptions. a)  $(B-V)_{\max}^{00}$  of SN 1986G is given by equation (1) like normal SNe Ia, and b) it has the tail color  $(B-V)_{35}^{00} = 1.067$  which, from equation (2), is the tail color of a normal SN with  $\Delta m_{15} = 1.69$ . The results for both cases are shown in Table 7. In the latter case, with the tail color as standard, the extinction  $E(B-V)_{\max 35}$  becomes 0.489, which seems on the low side given its position in a prominent dust lane. However, even the small reddening makes SN 1986G bluer than average SNe-91bg and its relatively slow decline rate ( $\Delta m_{15} = 1.69$ ) remains untypical for this class, although with the distance modulus of NGC 5128 of  $(m - M)^0 = 27.80$  (Thim et al. 2003) its absolute magnitudes  $M_{BV}$  become quite similar to SNe-91bg. On the other hand case a) leads to  $E(B-V)_{\text{host}} = 0.922$  and  $E(B-V)_{\text{total}} = 1.037$  (including Galactic reddening) in good agreement with the independent estimates of Rich (1987) and Cristiani et al. (1992). Hence, we prefer solution a) and conclude that the luminosity of SN 1986G lies inbetween normal SNe Ia and SNe-91bg (see Table 7).

An overview of the luminosity distribution in  $B$  of the various types of SNe Ia is given in Figure 14.

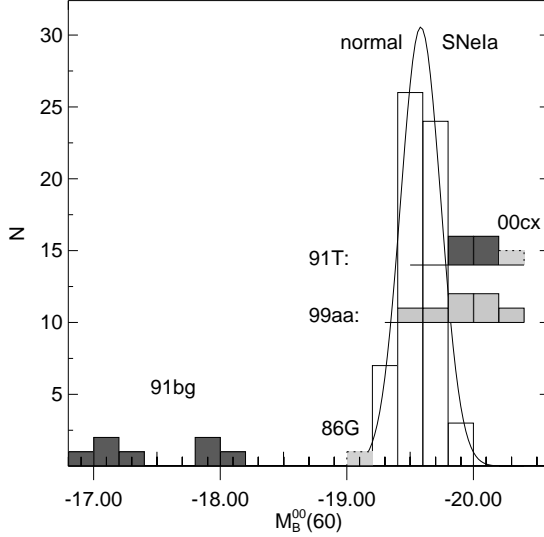


Fig. 14.— The distribution in absolute magnitude  $M_B^{00}$  of SNe Ia. The 58 normal SNe Ia of the fiducial sample, normalized for  $\Delta m_{15}$  and  $(B-V)_{\max}^{00}$ , are shown in the open histogram with a fitted Gauss curve. The spectroscopically peculiar SNe-91bg and SNe-91T are in dark grey, the SNe-99aa in light grey. In addition the unusual SN 1986G and 2000cx are shown.

## 8. THE HUBBLE DIAGRAM OF NORMAL SNe Ia

The Hubble diagram –  $\log cz$  vs.  $m_{BVI}^{\text{corr}}$  – is shown in Figure 15 for 108 normal SNe Ia. The recession velocities are corrected for streaming motions as described in the explanation of column 5 of Table 1 (§ 2). The apparent magnitudes are corrected for Galactic and host galaxy absorption as laid out in § 5 and reduced to  $\Delta m_{15} = 1.1$  and  $(B-V)_{\max}^{00} = -0.024$  (equation 23).

A slightly curved Hubble line, corresponding to a flat Universe with  $\Omega_\Lambda = 0.7$ , is fitted to the points in Figure 15. The corresponding relation is given by Carroll et al. (1992)

$$\phi(z) = 0.2m_\lambda^{\text{corr}} + C_\lambda, \quad (24)$$

where

$$\phi(z) = \log c(1+z_1) \int_0^{z_1} [(1+z)^2(1+0.3z) - 0.7z(2+z)]^{-1/2} dz, \quad (25)$$

and where the intercept is given by

$$C_\lambda = \log H_0 - 0.2M_\lambda^{\text{corr}} - 5. \quad (26)$$

From this follows the decisive relation

$$\log H_0 = 0.2M_\lambda^{\text{corr}} + C_\lambda + 5. \quad (27)$$

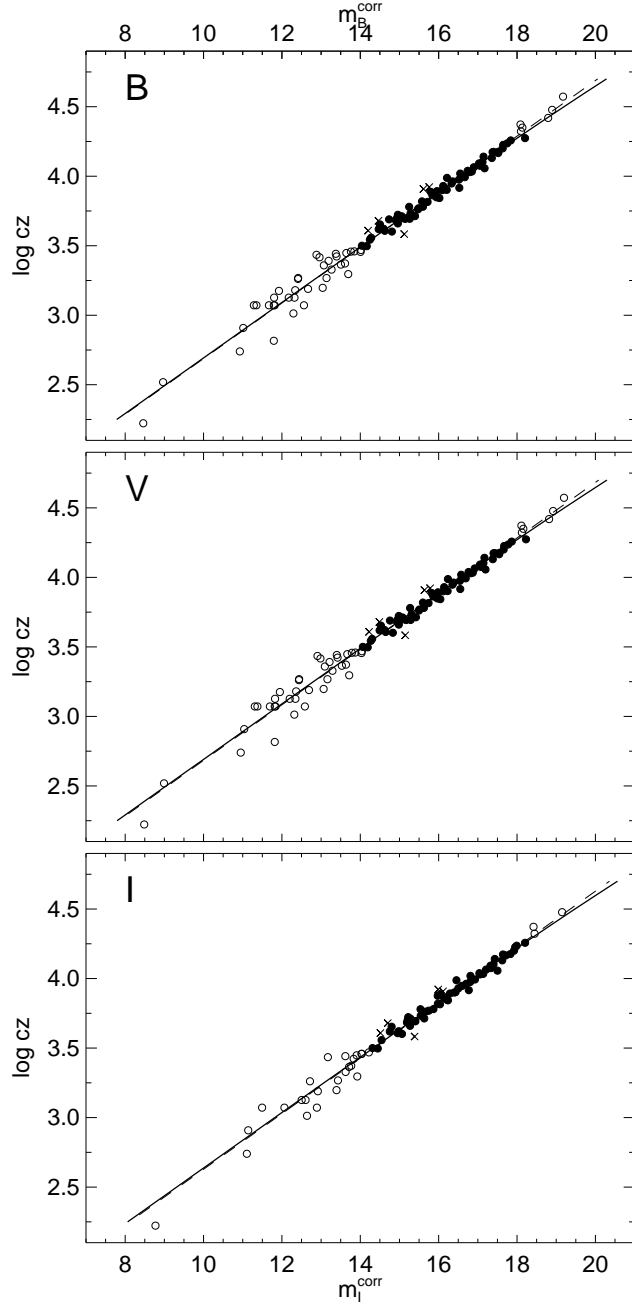


Fig. 15.— The Hubble diagram in  $B$ ,  $V$ , and  $I$  of 108 normal SNe Ia. The  $\Omega_M = 0.3$ ,  $\Omega_\Lambda = 0.7$  fits to the Hubble line in each color as given in Table 8 do not use five SNe Ia (plotted with  $\times$ ) discussed in § 5.2. The SNe Ia with  $v < 3000 \text{ km s}^{-1}$  and  $v > 20000 \text{ km s}^{-1}$  are shown as open symbols. The dashed line corresponds to a flat matter-dominated Universe.

Table 8. Nine solutions of  $C_\lambda$  in equation (27) for different choices of the SNeIa sample.

	$C_B$	$\sigma_B$	$C_V$	$\sigma_V$	$N_{BV}$	$C_I$	$\sigma_I$	$N_I$
1) all:	$0.696 \pm 0.006$	0.30	$0.691 \pm 0.006$	0.30	105	$0.634 \pm 0.006$	0.27	85
2) $v > 3000 [\text{km s}^{-1}]$ :	$0.697 \pm 0.004$	0.16	$0.693 \pm 0.004$	0.16	68	$0.640 \pm 0.004$	0.15	61
3) $3000 < v < 20000$ :	$0.693 \pm 0.004$	0.14	$0.688 \pm 0.004$	0.14	62	$0.637 \pm 0.004$	0.14	58
4) $v < 2000$ :	$0.675 \pm 0.021$	0.51	$0.670 \pm 0.021$	0.51	23	$0.590 \pm 0.025$	0.47	14
5) $v < 1200$ :	$0.656 \pm 0.034$	0.59	$0.651 \pm 0.034$	0.59	12	$0.583 \pm 0.045$	0.60	7
6) $v > 3000, E_t < 0.30$ :	$0.697 \pm 0.004$	0.16	$0.692 \pm 0.004$	0.16	63	$0.639 \pm 0.004$	0.15	58
7) $v > 3000, E_t < 0.15$ :	$0.697 \pm 0.005$	0.17	$0.693 \pm 0.005$	0.17	51	$0.638 \pm 0.005$	0.15	46
8) $v > 3000, E_t < 0.05$ :	$0.692 \pm 0.006$	0.16	$0.687 \pm 0.006$	0.16	24	$0.635 \pm 0.006$	0.15	21
9) $v > 5000$ , Table 2:	$0.695 \pm 0.007$	0.17	$0.692 \pm 0.006$	0.14	21	$0.640 \pm 0.005$	0.10	20

As equation (27) shows, the determination of  $H_0$  requires an independent calibration of  $M_\lambda^{\text{corr}}$  of normal SNeIa and an evaluation of the intercept  $C_\lambda$ . While a revised calibration of  $M_\lambda^{\text{corr}}$  will be provided in the forthcoming summary paper, the determination of  $C_\lambda$  is given here.

Nine solutions for  $C_\lambda$  are presented in Table 8 for different subsets of the SNeIa in Table 1a. The subsets are defined by velocity cuts and by different amounts of the total reddening  $E(B-V)_t$ .

It is very satisfactory that the solutions 1-3 and 6-8 for SNeIa beyond  $3000 \text{ km s}^{-1}$  give the same values for  $C_\lambda$  in each waveband within the statistical errors.  $C_B$  varies by  $\pm 0.003$  implying a variation in mean absolute magnitude  $\langle M_B^{\text{corr}} \rangle$  of only  $\pm 0.015$  mag, which influences  $H_0$  by less than  $\pm 1\%$ .

Solution 3 is from the fiducial sample as defined in § 5.2. It is least affected by photometric errors, peculiar motions, possibly remaining errors of the K-correction, and cosmological effects. The corresponding values of  $C_{BVI}$  with equation (26) and  $H_0 = 60$  give

$$M_B^{\text{corr}} = -19.57 \pm 0.02, \quad M_V^{\text{corr}} = -19.55 \pm 0.02, \quad \text{and} \quad M_I^{\text{corr}} = -19.29 \pm 0.02. \quad (28)$$

It is also noted that  $C_B - C_V = 0.005 \pm 0.006$  corresponding to  $(B-V)^{00} = -0.025 \pm 0.03$ , and that  $C_V - C_I = 0.051 \pm 0.006$  corresponding to  $(V-I)^{00} = -0.26 \pm 0.03$ , – both values being consistent with the observed colors in equation (4).

The solutions 6-8 admit different amounts of the total extinction  $E(B-V)_t$  in the Galaxy and in the host galaxy. This has virtually no effect on  $C_I$ , and even  $C_B$ , which is most sensitive to absorption corrections, changes by not more than 0.005 (corresponding to 0.025 mag). This proves in favor of the adopted unconventional values of  $\mathcal{R}_{BVI}$  (equation 13). The SNeIa in Table 1a have  $\langle E(B-V)_t \rangle = 0.16$ , and an error of  $\mathcal{R}_B$  of more than  $\Delta \mathcal{R}_B \approx \pm 0.25$  would cause a larger discrepancy. The limitation of the maximum value of  $E(B-V)_t$  does not lead to a decrease of the scatter about the Hubble line. This suggest that the

magnitude dispersion is mainly due to *random* errors of  $E(B-V)_t$  and of the corresponding absorption corrections.

If one averages the  $B$ ,  $V$ , and  $I$  magnitudes to define the Hubble line in solutions 1-8, the scatter is *not* reduced, which indicates that the magnitude errors are strongly correlated.

It is not meaningful to compare the values of  $C_{BVI}$  derived here with those of other authors, because they depend on a number of choices taken here: the intrinsic color of SNe Ia, the reddening and absorption law, and the reduction to the standard values of  $\Delta m_{15} = 1.1$  and  $(B-V)_{\max}^{00} = -0.024$ . It is therefore mandatory, if the present values of  $C_\lambda$  are to be used to obtain  $H_0$  through equation (27), that the calibrating SNe Ia are treated according to the prescriptions given here.

The dispersion about the Hubble line in solution 3, i.e.  $\sigma_{BVI} = 0.14$  mag, is quite satisfactory for a large sample of 62 (58) SNe Ia. Tripp (1998) has found from 29 SNe Ia  $\sigma_B = 0.15$  mag, but his reddening-to-absorption ratio of  $\mathcal{R}_B = 2.09$  for Galactic and host galaxy absorption seems unrealistic. Previous values of  $\sigma_V = 0.14$  (Hamuy et al. 1996b; Phillips et al. 1999) or even  $\sigma_V = 0.12$  mag (Parodi et al. 2000) are based on smaller samples, and are in addition color-limited by  $(B-V)_{\max} \leq 0.2$ . Altavilla et al. (2004) have found  $\sigma_B = 0.20$  mag for 18 of their low-extinction SNe Ia. For comparison the MLCS method of fitting the SN light curves has yielded  $\sigma_V = 0.16$  (Riess et al. 1999; Jha et al. 1999) and  $\sigma_V = 0.20$  mag (Tonry et al. 2003). The “Bayesian Adapted Template Match” (BATM) of Barris & Tonry (2004) yields a scatter of  $\sigma_{(m-M)} = 0.21$  mag. The very small scatter of  $\sigma = 0.08$  mag achieved by Wang et al. (2003) with their “Color-Magnitude Intercept Calibration” may not be representative because it is derived from a severely color-restricted sample; their color limit  $(B-V)_{\max}^0 \leq 0.05$  cuts into the realistic color distribution of even unreddened SNe Ia (cf. Figure 1).

A physically more relevant question concerns the *intrinsic* scatter of homogenized SN luminosities. The best handle for this is offered by the 21 (20) SNe Ia in Table 2 with minimum absorption in their host galaxies and  $v > 5000 \text{ km s}^{-1}$  (solution 9 of Table 8). The higher velocity limit is chosen here to guard against peculiar motions which, if  $\sim 300 \text{ km s}^{-1}$ , can contribute a magnitude dispersion of 0.2 mag still at  $v = 3000 \text{ km s}^{-1}$ . The sample gives a puzzlingly large value of  $\sigma_B = 0.17$ , but quite low values for  $\sigma_V = 0.14$  and  $\sigma_I = 0.10$  mag. The small scatter in  $I$  is particularly noteworthy because  $I_{\max}$ , occurring before  $B_{\max}$ , requires good photometry at an early phase. Allowing conservatively for an average photometric error of  $\sigma_m = 0.05$  mag, we derive an intrinsic scatter of the homogenized  $I_{\max}$  magnitudes of  $\lesssim 0.10$  mag, which – in view of the many small and not so small spectroscopic and light curve differences between normal SNe Ia – is remarkably small.

We have refrained from weighting the SN data, as some authors have done, by the quoted magnitude errors or by the time interval between inferred  $B$  maximum and the onset of the photometry, although these data are given for most, but not all SNeIa in Table 1a. The reason is mainly that the quoted magnitude errors from many different sources carry an subjective element, and that they include sometimes systematic errors and sometimes not. We have instead made alternative solutions excluding SNeIa with large quoted magnitude errors and/or with a late onset of their photometry. In no case the result or even the statistical error was significantly changed. In view of the large sample considered here this is no surprise.

A last comment to the solutions in Table 8 concerns the relative size of  $H_0$  in the local Universe. The strong increase of  $\sigma_{BVI}$  in solution 4 and 5 is certainly due to peculiar motions whose influence becomes important at small redshifts. The median velocity of the SNeIa in solution 4 is  $1200 \text{ km s}^{-1}$ . The observed magnitude scatter of  $\sigma_I = 0.47$  corresponds therefore to typical peculiar motions of  $\sim 280 \text{ km s}^{-1}$ . Within  $v < 1200 \text{ km s}^{-1}$  the median velocity is  $1000 \text{ km s}^{-1}$  and the scatter corresponds here to  $\sim 300 \text{ km s}^{-1}$ . These values are high relative to the small rms peculiar velocity of  $< 100 \text{ km s}^{-1}$  consistently derived over still smaller scales (e.g. Tammann & Sandage 1985; Sandage 1986, 1987; Karachentsev & Makarov 1996), but many of the SNeIa lie in the Virgo cluster region which is known to be noisy (Tammann et al. 2002), and peculiar velocities are generally expected to increase with increasing scale length up to some asymptotic value which, judging from the CMB dipole, is  $\gtrsim 630 : \sqrt{3} = 360 \text{ km s}^{-1}$  in the radial direction. – For  $v < 2000 \text{ km s}^{-1}$   $C_{BV}$  becomes smaller by  $0.018 \pm 0.021$  and  $C_I$  by  $0.047 \pm 0.025$  than in solution 3. This correspond from equation (27) to a local decrease of  $H_0$  by  $5 \pm 5\%$  or  $12 \pm 6\%$ . Analogously the very local value of  $H_0$  is, from solution 5,  $9 \pm 9\%$  or  $16 \pm 14\%$  smaller than the cosmic value. The local decrease of  $H_0$  is in view of the small number of SNeIa and the statistical errors only suggestive.

The mean absolute magnitude  $M_V^{\text{corr}}$  in equation (28) is combined with the individual apparent magnitudes  $m_V^{\text{corr}}$  in Table 3a, column 9, to yield photometric absorption-free distance moduli for 111 normal SNeIa and hence of their parent galaxies (Table 3a, column 11). The expected random error is only  $\sigma_{m-M} = 0.14$  mag; some moduli suspected for one reason or another to be less accurate are shown in parentheses. The moduli have the advantage – particularly for the nearby galaxies – to be independent of peculiar motions. Of course, all distances are still to be shifted by a constant amount, once the adopted value of  $H_0 = 60$  can be replaced by the actual value of  $H_0$ , which is the ultimate aim of this series.

## 9. SUMMARY AND CONCLUSIONS

The main purpose of this paper is to update an earlier summary by Parodi et al. (2000) on the reddening, absorption and second parameter corrections for a color-restricted sample of "Branch normal" type Ia supernovae where the corrected data were used to construct the Hubble diagram in  $B$ ,  $V$ , and  $I$ . Here the sample is increased to 124 type Ia supernovae with no restrictions placed on the observed color, thereby avoiding the criticisms of the Parodi et al. sample raised by others concerning observational selection biases.

All SN believed to be "Branch normal" (Branch et al. 1993) were used, together with 13 spectroscopically peculiar SNe Ia (types 91T, 91bg, SN 2000cx, 1986G) that deviate in one way or another from the main sample. The peculiar supernovae are listed separately in Tables 1b, 1c, 3b, and 3c and are discussed in § 7.

Because no a priori cut in observed color at maximum was imposed, many of the SNe in our enlarged sample suffer non-negligible reddening in their host galaxies, and care has been taken at each step in the reductions to guard against systematic errors in the derived absorptions.

The twelve main research points made in the paper are these.

(1) The 22 SNe Ia in E or S0 galaxies and the 12 SNe Ia in the outlying regions of spirals, set out in Table 2, are expected to have nearly negligible extinction due to the host galaxy. Their mean intrinsic colors, corrected for Galactic reddening and nearly free of any host galaxy reddening, are  $(B-V)_{\max}^{00} = -0.013$ ,  $(B-V)_{35}^{00} = 1.092$  (i.e. the tail color at phase  $t_B = 35^d$ ), and  $(V-I)_{\max}^{00} = -0.232$ . The individual colors  $(B-V)_{\max}^{00}$  become marginally redder, the colors  $(V-I)_{\max}^{00}$  significantly redder with increasing decline rate  $\Delta m_{15}$ , while the tail colors  $(B-V)_{35}^{00}$  become clearly bluer with increasing  $\Delta m_{15}$  (equations 1–3). The latter result is in variance with Lira (1995), Phillips et al. (1999), Jha (2002), and Altavilla et al. (2004), who assumed the tail colors to be independent of any second parameters.

(2) The host galaxy reddenings for all other normal SNe Ia in the sample are based on the intrinsic colors derived in item (1) above. The difference between the observed, Galactic-reddening-free colors  $(B-V)_{\max}^0$ ,  $(B-V)_{35}^0$ , and  $(V-I)_{\max}^0$  and the corresponding colors from equations (1–3), i.e. adjusted to the appropriate value of  $\Delta m_{15}$ , yield three different estimates of the reddening  $E(B-V)_{\max}$ ,  $E(B-V)_{35}$ , and  $E(V-I)_{\max}$ .

(3) Due to the general color dependence of color excesses caused by the photometric bandwidth effect, the excesses  $E(B-V)_{35}$ , determined in item (2) from a late, quite red phase of the SN light curves, must be converted to the value applicable at the blue maximum phase. This is achieved by requiring that  $(B-V)_{\max}^{00}$  as well as  $(V-I)_{\max}^{00}$  be independent of  $E(B-V)_{35}$

(cf. Figures 3 & 5). The requirement leads to equation (9) which converts  $E(B-V)_{35}$  to  $E(B-V)_{max35}$ , and to equation (11) which converts  $E(V-I)$  into  $E(B-V)_{max}^{V-I}$ . The three determinations of  $E(B-V)_{max}$  are intercompared in Figures 4 & 6. They agree well and are averaged to give the adopted reddening  $E(B-V)_{host}$  in the host galaxy. The random error of  $E(B-V)_{host}$  is 0.043 mag.

(4) The adopted color excesses  $E(B-V)_{host}$  depend on the assumption that the sample of SNe Ia in E/S0 galaxies and the outliers in spirals in Table 2 suffer no host-galaxy reddenings. If, in fact, they do suffer a non-zero amount of reddening, the true intrinsic colors of the complete sample, determined by the method of items (1) through (3), will be bluer, and the magnitudes brighter than adopted here, but this will have no effect on the calibration of  $H_0$  to be made in the final summary paper of this series as long as the calibrating SNe Ia in host galaxies are reduced to the *same* color. In that case, the local calibrators would suffer the same error in absorption as would the distant SNe Ia defining the global Hubble diagram, and the error cancels.

(5) The magnitudes  $m_{BVI_{max}}^0$ , corrected for conventional Galactic absorption, were transformed into absolute magnitudes  $M_{BVI_{max}}^0$  for a “fiducial” sample of 62 (58) SNe Ia which have  $3000 < v_{CMB} < 20\,000 \text{ km s}^{-1}$  (excluding only the highly absorbed SN 1996ai and five SNe Ia deviating by more than  $2\sigma$  and discussed in § 5.2) to guard against peculiar motions and other effects. A flat Universe with  $H_0 = 60$ ,  $\Lambda = 0.7$  was assumed. We show in § 5.2 a strong correlation of  $M_{BVI_{max}}^0$  with  $E(B-V)_{host}$  (Figure 9). This correlation determines the ratio of absorption-to-reddening in the host galaxy. The absorption-to-reddening values determined in this way are  $\mathcal{R}_B = 3.65 \pm 0.16$ ,  $\mathcal{R}_V = 2.65 \pm 0.15$ , and  $\mathcal{R}_I = 1.35 \pm 0.21$ . These well determined values differ significantly from the canonical values in the Galaxy of  $\mathcal{R}_{BVI}$  of 4.1, 3.1, and 1.8. The significant difference with the Galactic values has been pointed out before by Branch & Tamman (1992), Riess et al. (1996), Phillips et al. (1999), Krisciunas et al. (2000), Wang et al. (2003), and Altavilla et al. (2004). An explanation is that the intense radiation of the supernovae in some manner modifies the size distribution of the dust grains in the host galaxy near the SN. The canonical values of  $\mathcal{R}_{BVI}$  have been used to determine the Galactic absorption and the new, smaller values of  $\mathcal{R}_{BVI}$  for the absorption in the host galaxy.

(6) The absorption-free magnitudes  $M_V^{00}$  of the fiducial sample are plotted against the Hubble type of the host galaxies in Figure 10. It is confirmed that the supernovae in E/S0 galaxies average  $\sim 0.3$  magnitude fainter than SNe in late-type spirals, known already since 1995 (Hamuy et al. 1995; Saha et al. 1997, 1999; Sandage & Tamman 1997; Sandage et al. 2001, Figure 6). It has been seen in a different form by the discovery by Hamuy et al. (1996b, their Figure 4), that the decline rate,  $\Delta m_{15}$ , is correlated with galaxy type (SNe Ia in E/S0

galaxies have average decline rates near 1.5 mag, while those in late-type spirals have a mean rate near 1.0), coupled with the fact that the SNe Ia with large decline rates are fainter than those with smaller rates.

The reason for the  $M_{\max}^{00}$ -galaxy type correlation is expected to be related to the different gestation times for type Ia SNe and the subsequent difference in the Fe abundance between E/S0 galaxies and spirals of the same age. The consequences may or may not be profound in using SNe Ia for cosmological probes as is the current trend (Riess et al. 1998, 2004; Perlmutter et al. 1999; Knop et al. 2003; Barris et al. 2004), depending on the precision with which the effect can be compensated for by the  $\Delta m_{15}$  correlations with galaxy type.

(7) The fully absorption-corrected magnitudes  $M_{BVI}^{00}$  confirm the Pskovskii (1967) effect of a correlation with the  $\Delta m_{15}$  decline rates (Figure 11) with correlation slopes of  $\alpha_B = 0.619 \pm 0.076$ ,  $\alpha_V = 0.608 \pm 0.074$ ,  $\alpha_I = 0.438 \pm 0.076$  (Table 4).

The present slopes  $\alpha_{BVI}$ , which correct for the magnitude differences of SNe Ia in E/S0 galaxies and spirals, lie between the smaller values of Parodi et al. (2000) and the larger values of Phillips et al. (1999) and Altavilla et al. (2004). It is shown that the reason for this is the sensitivity of  $\alpha_{BVI}$  on the adopted slopes of the color- $\Delta m_{15}$  relation in equations (1–3). Steeper slopes of these relations lead necessarily to larger values of  $\alpha_{BVI}$ . Incorrect slopes of the color- $\Delta m_{15}$  relation enter the color excesses and propagate strongly into the absorption and hence into the  $M^{00}$  magnitudes. They cancel, however, if the latter are normalized to a common value of  $\Delta m_{15}$  ( $M_{15}^{00}$ ).

(8) The absolute magnitudes,  $M_{BVI\max}^{00}$  show some dependence on the  $(B-V)_{\max}^{00}$  and  $(V-I)_{\max}^{00}$  colors (Figure 12), as suggested by Tripp & Branch (1999) and Parodi et al. (2000). Therefore the adopted magnitudes  $M_{BV}^{\text{corr}}$  of normal SNe Ia have been reduced to common values of  $\Delta m_{15} = 1.1$  and  $(B-V)_{\max}^{00} = -0.024$  by equation (23) and Table 5. This slightly reduces the dispersion about the Hubble line without changing the *mean* magnitude of the sample.

(9) The present sample of 124 SNe Ia contains only four spectroscopically distinct SNe-91T, with SN 1991T as the prototype. Their apparent rarity must be real because of their pronounced overluminosity. The overluminosity amounts to  $\Delta M_B = -0.40 \pm 0.08$  on average if one assumes them to have the same color at maximum  $(B-V)_{\max}^{00}$  as normal SNe Ia (Table 6). The mean overluminosity is reduced to  $-0.32 \pm 0.08$  if one allows in addition for their below-average decline rates  $\Delta m_{15}$ .

The new class of SNe-99aa (Li et al. 2001b), named after SN 1999aa, comprises seven objects in Table 1a (marked with †). They are spectroscopically between normal SNe Ia and SNe-91T, but are difficult to recognize because their spectroscopic peculiarity is confined to

the pre-maximum phase. Their true frequency in a distance-limited sample may therefore be as high as  $\sim 14\%$ . They are less overluminous than SNe-91T, i.e.  $\Delta M_B = -0.30 \pm 0.10$ , or  $\Delta M_B = -0.19 \pm 0.10$  if reduced to  $\Delta m_{15} = 1.1$ , as compared to normal SNe Ia. – SNe-99aa have very slow decline rates ( $\langle \Delta m_{15} \rangle = 0.92$ ) and occur correspondingly in late-type galaxies. The mean coded type of their host galaxies is  $\langle T \rangle = 3.7 \pm 0.5$  ( $\sim$ Sbc) as compared to  $\langle T \rangle = 3.5 \pm 1.0$  for SNe-91T and  $\langle T \rangle = 1.8$  ( $\sim$ Sab) for normal SNe Ia.

The most luminous SN in the sample is probably the very peculiar SN 2000cx which has – with plausible absorption corrections –  $M_{BV}^{00} \approx -20.3$ .

(10) Seven SNe-91bg, whose eponymous star is SN 1991bg, have sufficient photometry to be included in Table 1c. They are very red and spectroscopically peculiar. In accordance with their exceptionally fast decline rates ( $\Delta m_{15} \geq 1.9$ ) they lie preferentially in early-type galaxies ( $\langle T \rangle = -0.6$ ). This suggests little absorption in their host galaxies; zero absorption is assumed here to derive their intrinsic photometric properties (Table 7). The SNe-91bg emerge as a surprisingly homogeneous and separate class with  $B$  magnitudes at maximum about 2 mag below that of normal SNe Ia. The luminosity of SN 1986G seems to lie between SNe Ia and SNe-91bg (see Table 7).

(11) The Hubble diagrams in  $B$ ,  $V$ , and  $I$  for all 111 normal SNe Ia in Table 1a are shown in Figure 15 using fully corrected apparent magnitudes  $m_{BVI}^{\text{corr}}$ . Solutions for the intercepts  $C_\lambda$  of the Hubble line are given for various subsets with different restrictions in Table 8. The fiducial sample of 62 (58) SNe Ia with  $3000 < v < 20000 \text{ km s}^{-1}$  is taken as the most reliable sample (solution 3 in Table 8). The resulting values of  $C_\lambda$  inserted in equation (27) and  $H_0 = 60$  give  $\langle M_B^{\text{corr}} \rangle = -19.57 \pm 0.02$ ,  $\langle M_V^{\text{corr}} \rangle = -19.55 \pm 0.02$ , and  $\langle M_I^{\text{corr}} \rangle = -19.29 \pm 0.02$ . The dispersion of the  $m_{BVI}^{\text{corr}}$  magnitudes (corrected for Galactic and internal absorption and normalized to  $\Delta m_{15} = 1.1$ ) about the Hubble line is  $\sigma_{BVI} = 0.14$  mag (solution 3 in Table 8). It increases for distances shorter than  $3000 \text{ km s}^{-1}$  due to peculiar motions (solutions 5 and 6). Much of the dispersion beyond  $3000 \text{ km s}^{-1}$  is caused by random errors of the host galaxy absorption, as seen by the SNe Ia with minimum absorption in Table 2 which give  $\sigma_I = 0.10$  mag, if restricted in addition to  $v > 5000 \text{ km s}^{-1}$ . This is for normal SNe Ia, after they are normalized to common values of  $\Delta m_{15}$  and  $(B-V)_{\text{max}}^{00}$ , an *upper* limit to their intrinsic luminosity dispersion in  $I$  in view of remaining observational magnitude errors. The intrinsic dispersion in  $B$  and  $V$  may be somewhat larger.

In spite of the noticeable scatter introduced by the corrections for host galaxy absorption, the *mean* of the corrections must be nearly correct. This is demonstrated by solutions 3 and 6-8 in Table 8, where different cuts of the accepted maximum value of the total color excess  $E(B-V)_t$  lead to statistically insignificant variations of the intercept  $C_\lambda$  of only  $\pm 0.004$  (corresponding to  $\pm 0.02$  mag).

The combination of the absolute magnitude  $M_V^{\text{corr}}$  from above with the individual apparent magnitudes  $m_V^{\text{corr}}$  yields the absorption-free luminosity distances of 111 parent galaxies of normal SNe Ia (Table 3a, column 11). The distances are particularly valuable for nearby galaxies because they are insensitive to peculiar motions. If the value  $H_0 = 60$  is to be replaced by any other value, the listed distance moduli need only a bulk correction by an additive term.

Had we adopted a flat Universe with  $\Omega_M = 1$  the value of  $C_\lambda$  in solution 3 of Table 8 would change by only  $-0.009$ . This would decrease  $H_0$  by merely 2%. The insensitivity of  $H_0$  to the cosmological model is due to the velocity cut at  $v_{\text{CMB}} < 20\,000 \text{ km s}^{-1}$  of solution 3.

(12) The main goal of the present paper is to determine an up-to-date Hubble diagram using a large and unbiased sample of Branch-normal SNe Ia, whose magnitudes are corrected for Galactic and host galaxy absorption and normalized to standard values of the decline rate  $\Delta m_{15}$  and of the color  $(B-V)_{\text{max}}^{00}$ . Regardless whether one considers the unrestricted sample of non-local or restricted samples with only a minimum of extinction one finds remarkably robust solutions for the intercept  $C_\lambda$ , which through equation (27) is decisive for the determination of the value of  $H_0$ . The remaining uncertainty of  $C_\lambda$  of  $\sim 0.004$  will carry an error into the derived value of  $H_0$  of only 1%. The consequence is that the accuracy of the derived large-scale value of  $H_0$  will depend almost exclusively on the goodness of the luminosity calibration that we can achieve in a forthcoming paper by means of the SNe Ia in host galaxies with known Cepheids.

We are greatly indebted to Dr. G. Altavilla for kindly providing his unpublished template-fitted  $V_{\text{max}}$  magnitudes for a large sample of SNe Ia. We are equally indebted to Dr. S. Jha for his generosity to make his unpublished tail colors  $(B-V)_{35}$  available to us. B. R. thanks an anonymous donator for financial support, while G. A. T. thanks the Swiss National Science Foundation for support over many decades. A. S. is indebted to the Carnegie Institution for ongoing post-retirement facilities support.

## REFERENCES

- Altavilla, G., et al. 2004, MNRAS, 349, 1344  
Anapuma, G.C. 1997, AJ, 114, 2054  
Barbon, R., Ciatti, F., & Rosino, L. 1973, A&A, 25, 241  
Barris, B.J., & Tonry, J.L. 2004, ApJ, 613, 21

- Barris, B.J., et al. 2004, *ApJ*, 602, 571
- Benetti, S., et al. 2004, *MNRAS*, 348, 261
- Berlind, P., Jha, S., Garnavich, P., & Kirshner, R. 1997, *IAU Circ.*, 6700, 2
- Bottari, C., Nakano, S., Kushida, Y., Garnavich, P., Challis, P., Kirshner, R., Berlind, P., & Kleyna, J. 1996, *IAU Circ.*, 6422
- Branch, D., & Tammann, G.A. 1992, *ARA&A*, 30, 359
- Branch, D., Fisher, A., & Nugent, P. 1993, *AJ*, 106, 2383
- Candia, P., et al. 2003, *PASP*, 115, 277
- Carroll, S.M., Press, W.H., & Turner, E.L. 1992, *ARA&A*, 30, 499
- Cristiani, S., et al. 1992, *A&A*, 259, 63
- Dale, D.A., & Giovanelli, R. 2000, in *ASP. Conf. Ser.* 201, *Cosmic Flows Workshop*, eds. S. Courteau & J. Willick (San Francisco: ASP), 25
- de Vaucouleurs, G., de Vaucouleurs, A., & Corwin, H.G. 1976, *Second Reference Catalogue of Bright Galaxies* (Austin: Univ. of Texas Press)
- Federspiel, M., Sandage, A., & Tammann, G.A. 1994, *ApJ*, 430, 29
- Filippenko, A.V., et al. 1992, *ApJ*, 384, L15
- Fisher, A., Branch, D., Hatano, K., & Baron, E. 1999, *MNRAS*, 304, 67
- Garavini, G., et al. 2004, *AJ*, 128, 387
- Garnavich, P.M., et al. 2004, *ApJ*, 613, 1120
- Germany, L.M., Reiss, D.J., Schmidt, B.P., Stubbs, C.W., & Suntzeff, N.B. 2004, *A&A*, 415, 863
- Hamuy, M., Phillips, M.M., Maza, J., Suntzeff, N.B., Schommer, R.A., & Aviles, R. 1995, *AJ*, 109, 1
- Hamuy, M., Phillips, M.M., Suntzeff, N.B., Schommer, R.A., Maza, J., & Aviles, R. 1996a, *AJ*, 112, 2391
- Hamuy, M., Phillips, M.M., Suntzeff, N.B., Schommer, R.A., Maza, J., & Aviles, R. 1996b, *AJ*, 112, 2398

- Hamuy, M., Phillips, M.M., Suntzeff, N.B., Schommer, R.A., Maza, J., Smith, R.C., Lira, P., & Aviles, R. 1996c, AJ, 112, 2438
- Hamuy, M., Trager, S.C., Pinto, P.A., Phillips, M.M., Schommer, R.A., Ivanov, V., & Suntzeff, N.B. 2000, AJ, 120, 1479
- Hamuy, M., et al. 1996d AJ, 112, 2408
- Höflich, P., Gerady, C.L., Fesen, R.A., & Sakai, S. 2002, ApJ, 568, 791
- Howell, D.A. 2001, ApJ, 554, L193
- Jha, S. 2002, PhD. thesis, Harvard Univ.
- Jha, S., et al. 1999, ApJS, 125, 73
- Karachentsev, I.D., & Makarov, D.A. 1996, AJ, 111, 794
- Knop, R.A., et al. 2003, ApJ, 598, 102
- Kowal, C.T. 1968, AJ, 73, 1021
- Kraan-Korteweg, R.C. 1986, A&AS, 66, 255
- Krisciunas, K., Hastings, N.C., Loomis, K., McMillan, R., Rest, A., Riess, A.G., & Stubbs, C. 2000, ApJ, 539, 658
- Krisciunas, K., et al. 2001, AJ, 122, 1616
- Krisciunas, K., et al. 2003, AJ, 125, 166
- Li, W., Filippenko, A.V., & Riess, A.G. 2001a, ApJ, 546, 719
- Li, W., Filippenko, A.V., Treffers, R.R., Riess, A.G., Hu, J., & Qiu, Y. 2001b, ApJ, 546, 734
- Li, W., et al. 2001c, PASP, 113, 1178
- Li, W.D., et al. 1999, AJ, 117, 2709
- Lira, P. 1995, Master Thesis, Univ. Chile
- Macri, L.M., Stetson, P.B., Bothun, G.D., Freedman, W.L., Garnavich, P.M., Jha, S., Madore, B.F., & Richmond, M.W. 2001, ApJ, 559, 243
- Mandel, K., Jha, S., Matheson, T., Challis, P., & Kirshner, R.P. 2001, BAAS, 33, 1370

- Mazzali, P.A., Chugai, N., Turatto, M., Lucy, L.B., Danziger, I.J., Cappellaro, E., della Valle, M., & Benetti, S. 1997, MNRAS, 284, 151
- Nobili, S., Goobar, A., Knop, R., & Nugent, P. 2003, A&A, 404, 901
- Parodi, B.R., Saha, A., Sandage, A., & Tammann, G.A. 2000, ApJ, 540, 634
- Perlmutter, S., et al. 1997, ApJ, 483, 565
- Perlmutter, S., et al. 1999, ApJ, 517, 565
- Phillips, M.M. 1993, ApJ, 413, L105
- Phillips, M.M., Lira, P., Suntzeff, N.B., Schommer, R.A., Hamuy, M., & Maza, J. 1999, AJ, 118, 1766
- Pignata, G., et al. 2004, MNRAS, in press (astro-ph/0408234)
- Pskovskii, Y.P. 1967, Sov. Astron., 11, 63
- Pskovskii, Y.P. 1971, Sov. Astron., 14, 798
- Pskovskii, Y.P. 1984, Sov. Astron., 28, 658
- Rich, R.M. 1987, AJ, 94, 651
- Riess, A.G., Press, W.H., & Kirshner, R.P. 1996, ApJ, 473, 88
- Riess, A.G., et al. 1998, AJ, 116, 1009
- Riess, A.G., et al. 1999, AJ, 117, 707
- Riess, A.G., et al. 2004, ApJ, 607, 665
- Saha, A., Sandage, A., Labhardt, L., Tammann, G.A., Macchetto, F.D., & Panagia, N. 1996, ApJS, 107, 693 (SN 1960F)
- Saha, A., Sandage, A., Labhardt, L., Tammann, G.A., Macchetto, F.D., & Panagia, N. 1997, ApJ, 486, 1 (SN 1990N)
- Saha, A., Sandage, A., Tammann, G.A., Dolphin, A.E., Christensen, J., Panagia, N., & Macchetto, F.D. 2001b, ApJ, 562, 314 (SN 1998aq)
- Saha, A., Sandage, A., Tammann, G.A., Labhardt, L., Macchetto, F.D., & Panagia, N. 1999, ApJ, 522, 802 (SN 1989B)

- Saha, A., Sandage, A., Thim, F., Labhardt, L., Tammann, G.A., Christensen, J., Panagia, N., & Macchetto, F. D. 2001a, *ApJ*, 551, 973 (SN 1991T)
- Sandage, A. 1986, *ApJ*, 307, 1
- Sandage, A. 1987, *ApJ*, 317, 557
- Sandage, A., & Tammann, G.A. 1982, *ApJ*, 256, 339
- Sandage, A., & Tammann, G.A. 1993, *ApJ*, 415, 1
- Sandage, A., & Tammann, G.A. 1995, *ApJ*, 446, 1
- Sandage, A., & Tammann, G.A. 1997, in *Critical Dialogues in Cosmology*, ed. N. Turok (Singapore: World Scientific), 130
- Sandage, A., Tammann, G.A., & Reindl, B. 2004, *A&A*, 424, 43
- Sandage, A., Tammann, G.A., & Saha, A. 2001, in *Supernovae and gamma-ray bursts: the greatest explosions since the Big Bang*, eds. M. Livio, N. Panagia, & K. Sahu (Cambridge: Cambridge University Press), 304
- Schaefer, B.E. 1998, *ApJ*, 509, 80
- Schlegel, D., Finkbeiner, D., & Davis, M. 1998, *ApJ*, 500, 525
- Stritzinger, M., et al. 2002, *AJ*, 124, 2100
- Strolger, L.-G., et al. 2002, *AJ*, 124, 2905
- Tammann, G.A., Reindl, B., Thim, F., Saha, A., & Sandage, A. 2002, in *ASP Conf. Ser.* 283, *A New Era in Cosmology*, eds. T. Shanks & N. Metcalfe (San Francisco: ASP), 258
- Tammann, G.A., & Sandage, A. 1985, *ApJ*, 294, 81
- Tammann, G.A., Sandage, A., & Reindl, B. 2003, *A&A*, 404, 423
- Thim, F., Tammann, G.A., Saha, A., Dolphin, A., Sandage, A., Tolstoy, E., & Labhardt, L. 2003, *ApJ*, 590, 256
- Tonry, J.L., et al. 2003, *ApJ*, 594, 1
- Tripp, R. 1998, *A&A*, 331, 815

- Tripp, R., & Branch, D. 1999, ApJ, 525, 209
- Valentini, G., et al. 2003, ApJ, 595, 779
- van den Bergh, S., Li, W., & Filippenko, A.V. 2002, PASP, 114, 820
- van den Bergh, S., Li, W., & Filippenko, A.V. 2003, PASP, 115, 1280
- Vinkó, J., et al. 2003, A&A, 397, 115
- Wang, L., Goldhaber, G., Aldering, G., & Perlmutter S. 2003, ApJ, 590, 944
- Wells, L.A., et al. 1994, AJ, 108, 2233

Table 1. Observed parameters of SNe Ia.

SN	Galaxy	T	$v_{\text{hel}}$	$v_{\text{CMB}/220}$	$B_{\text{max}}$	$V_{\text{max}}$	$I_{\text{max}}$	$\Delta m_{15}$	$E(B-V)$ Gal	$E(B-V)$ max	$E(B-V)$ max35	$E(B-V)$ $V-I$	Ref.
(1)	(2)	(3)	(4)	(5)	(6)	(7)	(8)	(9)	(10)	(11)	(12)	(13)	(14)
(a) normal SNe Ia													
1937C	IC 4182*	5	321	330 <sup>V</sup>	8.80	8.82	...	0.85	0.014	0.001	-0.045	...	A
1960F	NGC 4496A*	5	1730	1179 <sup>V</sup>	11.60	11.51	...	0.87	0.025	0.099	...	...	Sa
1972E	NGC 5253*	5	404	167 <sup>V</sup>	8.49	8.49	8.80	1.05	0.056	-0.030	-0.052	-0.069	Sa
1972J	NGC 7634	-1	3225	2855	14.80	14.56	...	1.45	0.046	0.202	-0.040	...	A
1974G	NGC 4414*	5	716	655 <sup>V</sup>	12.48	12.30	...	1.11	0.019	0.184	0.137	...	S
1980N	NGC 1316	1	1760	1338 <sup>F</sup>	12.49	12.42	12.70	1.30	0.021	0.064	0.039	-0.045	HA
1981B	NGC 4536*	4	1808	(1179 <sup>V</sup> )	12.04	11.98	...	1.13	0.018	0.064	0.009	...	A
1981D	NGC 1316	1	1760	1338 <sup>F</sup>	12.59	12.40	...	...	0.021	0.242	...	...	P
1982B	NGC 2268	4	2222	2610 <sup>V</sup>	13.65	13.40	...	0.94	0.064	0.217	0.041	...	A
1983G	NGC 4753	-1	1239	1497 <sup>V</sup>	13.00	12.80	...	1.30	0.034	0.180	0.281	...	A
1984A	NGC 4419	1	-261	1179 <sup>V</sup>	12.50	12.30	...	...	0.033	0.240	...	...	H
1989B	NGC 3627*	3	727	549 <sup>V</sup>	12.34	11.99	11.70	1.31	0.032	0.332	0.298	0.302	W
1990N	NGC 4639*	3	1010	1179 <sup>V</sup>	12.75	12.73	12.95	1.05	0.026	0.020	0.070	0.012	HA
1990O	MCG 3-44-03	1	9193	9175	16.59	16.51	16.80	0.94	0.093	0.018	-0.001	-0.076	HA
1990T	PGC 63925	1	11992	11893	17.27	17.35	17.36	1.13	0.053	-0.111	0.055	0.114	HA
1990Y	Anon 0335-33	-3	11702	11603	17.69	17.42	17.57	1.13	0.008	0.284	0.205	0.063	HA
1990af	Anon 2135-62	-1	15080	14966	17.91	17.84	...	1.59	0.035	0.036	-0.022	...	H
1991S	UGC 5691	3	16489	16807	17.78	17.75	17.99	1.00	0.026	0.032	0.033	0.004	HA
1991U	IC 4232	4	9426	9724	16.67	16.61	16.62	1.11	0.062	0.021	0.056	0.108	HA
1991ag	IC 4919	3	4264	4161	14.67	14.56	14.83	0.87	0.062	0.082	-0.012	-0.032	HA
1992A	NGC 1380	0	1877	1338 <sup>F</sup>	12.56	12.55	12.80	1.47	0.018	-0.001	-0.032	-0.040	HA
1992J	Anon 1009-26	-2	13491	13828	17.88	17.76	17.88	1.69	0.057	0.060	0.032	-0.011	HA
1992P	IC 3690	1	7615	7941	16.14	16.16	16.40	1.05	0.021	-0.015	0.014	0.003	HA
1992ae	Anon 2128-61	-3	22484	22366	18.62	18.54	...	1.30	0.036	0.059	0.053	...	A
1992ag	ESO 508-G67	5	7795	8095	16.64	16.47	16.50	1.20	0.097	0.092	0.359	0.059	HA
1992al	ESO 234-G69	3	4197	4048	14.59	14.65	14.93	1.09	0.034	-0.070	-0.015	-0.036	HA
1992aq	Anon 2304-37	1	30279	30014	19.42	19.39	19.48	1.69	0.012	0.015	0.026	0.044	HA
1992au	Anon 0010-49	-3	18287	18092	18.17	18.13	18.51	1.69	0.017	0.020	-0.014	-0.141	HA
1992bc	ESO 300-G9	2	5996	5876	15.13	15.25	15.56	0.90	0.022	-0.109	-0.108	-0.027	HA
1992bg	Anon 0741-62	1	10793	10936	17.39	17.30	17.32	1.15	0.185	-0.074	-0.015	-0.002	HA
1992bh	Anon 0459-58	4	13491	13519	17.68	17.63	17.75	1.13	0.022	0.050	0.061	0.070	HA
1992bk	ESO 156-G8	-3	17284	17237	18.07	18.14	18.21	1.67	0.015	-0.087	-0.018	0.056	HA
1992bl	ESO 291-G11	0	12891	12661	17.34	17.37	17.59	1.56	0.011	-0.038	-0.033	-0.024	HA
1992bo	ESO 352-G57	-2	5396	5164	15.86	15.84	15.95	1.69	0.027	-0.010	-0.030	0.020	HA
1992bp	Anon 0336-18	-2	23684	23557	18.53	18.53	18.68	1.52	0.069	-0.064	0.020	-0.024	HA
1992br	Anon 0145-56	-3	26382	26259	19.34	19.27	...	1.69	0.026	0.041	-0.020	...	H
1992bs	Anon 0329-37	3	18887	18787	18.33	18.33	...	1.15	0.011	0.010	0.017	...	A
1993B	Anon 1034-34	3	20686	21011	18.71	18.65	18.71	1.30	0.079	-0.004	0.122	0.045	HA
1993H	ESO 445-G66	2	7257	7522	16.99	16.72	16.60	1.69	0.060	0.207	0.022	0.137	HA
1993L	IC 5270	4	1926	1854 <sup>V</sup>	13.40	13.22	...	1.47	0.014	0.173	0.212	...	A
1993O	Anon 1331-33	-2	15589	15867	17.79	17.86	17.99	1.26	0.053	-0.107	-0.012	0.026	HA
1993ac	PGC 17787	-3	14690	14674	18.42	18.25	18.12	1.25	0.163	0.024	-0.004	0.101	RPA
1993ae	IC 126	-3	5712	5410	15.42	15.52	15.65	1.47	0.038	-0.131	-0.058	0.019	RPA
1993ag	Anon 1003-35	-2	14700	15013	18.30	18.12	18.22	1.30	0.112	0.082	0.055	-0.007	HA
1993ah	ESO 471-G27	-1	8803	8504	16.32	16.36	16.65	1.45	0.020	-0.052	0.048	-0.065	HA
1994D	NGC 4526	-1	448	1179 <sup>V</sup>	11.86	11.94	12.11	1.31	0.022	-0.088	-0.054	0.022	HA
1994M	NGC 4493	-3	6943	7289	16.35	16.30	16.40	1.45	0.023	0.035	0.083	0.052	RPA
1994Q	PGC 59076	-1	8863	8861	16.44	16.36	16.63	0.90	0.017	0.096	0.007	0.002	RPA

Table 1—Continued

SN	Galaxy	T	$v_{\text{hel}}$	$v_{\text{CMB}/220}$	$B_{\text{max}}$	$V_{\text{max}}$	$I_{\text{max}}$	$\Delta m_{15}$	$E(B-V)$ Gal	$E(B-V)$ max	$E(B-V)$ max35	$E(B-V)$ $V-I$	Ref.
(1)	(2)	(3)	(4)	(5)	(6)	(7)	(8)	(9)	(10)	(11)	(12)	(13)	(14)
1994S	NGC 4495	3	4550	4831	14.79	14.83	15.14	1.02	0.021	-0.034	-0.055	-0.038	R
1994T	PGC 46640	1	10390	10703	17.35	17.23	17.38	1.45	0.029	0.099	0.028	0.016	RPA
1994ae	NGC 3370	5	1279	1575 <sup>v</sup>	13.15	13.10	13.40	0.87	0.030	0.054	0.070	-0.025	RPA
1995D	NGC 2962	0	1966	2129 <sup>v</sup>	13.44	13.40	13.70	1.03	0.058	0.009	0.028	-0.063	RPA
1995E	NGC 2441	3	3470	3496	16.82	16.10	...	1.19	0.027	0.712	0.582	...	RA
1995ak	IC 1844	1	6811	6589	16.09	16.10	16.21	1.45	0.038	-0.040	0.172	0.033	RPA
1995al	NGC 3021	4	1541	1851 <sup>v</sup>	13.36	13.25	13.50	0.89	0.014	0.129	0.066	0.018	RPA
1996C	MCG 8-25-47	1	8094	8245	16.59	16.56	16.77	0.94	0.013	0.048	-0.007	0.039	RPA
1996X	NGC 5061	-3	2039	2120 <sup>v</sup>	13.26	13.21	13.39	1.32	0.069	-0.005	-0.016	-0.024	RPA
1996Z	NGC 2935	3	2277	2285 <sup>v</sup>	14.61	14.25	...	1.22	0.064	0.314	0.350	...	R
1996ab	Anon 1521+28	5	37240	37370	19.54	19.42	...	0.87	0.032	0.122	0.080	...	R
1996af <sup>1)</sup>	NGC 5005	4	946	1298 <sup>v</sup>	16.96	15.26	...	0.85	0.014	1.721	1.501	...	RA
1996bk	NGC 5308	-1	2041	2462 <sup>v</sup>	14.84	14.41	...	1.69	0.018	0.409	0.207	...	RA
1996bl	Anon 0036+11	5	10793	10447	17.08	16.98	17.03	1.11	0.092	0.031	0.036	0.059	RPA
1996bo	NGC 673	5	5182	4893	16.15	15.78	...	1.30	0.077	0.307	0.206	...	RA
1996bv	UGC 3432	5	4998	5016	15.77	15.54	15.56	0.84	0.105	0.160	0.098	0.092	RPA
1997E	NGC 2258	-1	4001	3998	15.59	15.45	15.46	1.39	0.124	0.026	0.013	0.031	J
1997Y	NGC 4675	3	4806	4964	15.28	15.30	15.36	1.25	0.017	-0.020	0.024	0.100	J
1997bp	NGC 4680	3	2492	2647 <sup>v</sup>	14.12	13.92	14.09	0.97	0.044	0.185	0.286	0.036	AJ
1997bq	NGC 3147	4	2820	2879	14.57	14.27	14.37	1.01	0.024	0.304	0.082	0.092	J
1997cw <sup>†</sup>	NGC 105	2	5133	4782	16.00	15.52	15.33	1.02	0.073	0.434	0.335	0.233	J
1997dg	anonymous	1	10193	9845	17.20	17.11	17.14	1.13	0.078	0.034	...	0.081	J
1997do	UGC 3845	4	3034	3140	14.56	14.46	14.59	0.99	0.063	0.065	...	0.044	J
1997dt	NGC 7448	4	2194	2356 <sup>v</sup>	15.64	15.08	14.54	1.04	0.057	0.529	...	0.463	J
1998V	NGC 6627	3	5268	5148	15.88	15.71	15.62	1.06	0.196	-0.001	-0.018	0.066	J
1998ab <sup>†</sup>	NGC 4704	5	8134	8354	15.94	15.93	15.98	0.88	0.017	0.026	0.070	0.141	J
1998aq	NGC 3982*	3	1109	1514 <sup>v</sup>	12.22	12.28	...	1.12	0.014	-0.051	-0.053	...	Sa
1998bu	NGC 3368*	2	897	810 <sup>v</sup>	12.22	11.86	11.65	1.15	0.025	0.356	0.209	0.272	A
1998dh	NGC 7541	5	2678	2766 <sup>v</sup>	14.24	13.98	14.04	1.23	0.068	0.210	0.090	0.061	J
1998dk	UGC 139	5	3963	3609	14.93	14.74	14.81	1.05	0.044	0.172	0.127	0.091	J
1998dm	MCG-01-4-44	4	1968	1976 <sup>v</sup>	14.70	14.48	14.28	1.07	0.044	0.201	0.259	0.258	J
1998dx	UGC 11149	-3	14990	14895	17.71	17.74	17.86	1.55	0.041	-0.068	...	0.015	J
1998ec	UGC 3576	3	5966	6032	16.44	16.21	16.22	1.08	0.085	0.169	...	0.092	J
1998ef	UGC 646	3	5319	5020	15.21	15.18	15.28	0.97	0.073	-0.014	...	0.056	J
1998eg	UGC 12133	5	7423	7056	16.62	16.50	16.49	1.15	0.123	0.018	...	0.067	J
1998es <sup>†</sup>	NGC 632	2	3168	2868	13.99	13.87	14.11	0.87	0.032	0.122	0.031	0.011	J
1999X	CGCG 180-22	...	7503	7720	16.45	16.29	16.31	1.11	0.032	0.151	...	0.126	J
1999aa <sup>†</sup>	NGC 2595	5	4330	4572	14.92	14.88	15.24	0.85	0.040	0.035	-0.033	-0.069	AJ
1999ac <sup>†</sup>	NGC 6063	4	2848	2944	14.34	14.28	14.32	1.00	0.046	0.042	...	0.113	J
1999aw	Anon 1101-06	...	11992	12363	16.86	16.84	17.24:	0.81	0.032	0.025	-0.076	-0.083	SIA
1999cc	NGC 6038	5	9392	9452	16.85	16.82	17.03	1.46	0.023	0.014	...	-0.018	J
1999cl	NGC 4501	3	2281	1179 <sup>V</sup>	15.11	13.89	13.08	1.19	0.038	1.201	...	0.634	J
1999dk	UGC 1087	5	4485	4181	15.04	14.95	15.22	1.28	0.054	0.051	0.084	-0.064	KA
1999dq <sup>†</sup>	NGC 976	5	4295	4060	14.88	14.68	14.76	0.88	0.110	0.123	0.119	0.047	J
1999ee	IC 5179	4	3422	3163	14.93	14.61	14.66	0.92	0.020	0.332	0.237	0.135	St
1999ef	UGC 607	5	11733	11402	17.52	17.39	17.69	1.06	0.087	0.068	...	-0.089	J
1999ej	NGC 495	0	4114	3831	15.65	15.60	15.66	1.41	0.071	-0.011	...	0.041	J
1999ek	UGC 3329	4	5253	5278	17.97	17.19	16.54	1.13	0.561	0.241	...	0.113	J
1999gd	NGC 2623	...	5535	5775	17.02	16.61	16.27	1.14	0.041	0.391	...	0.342	J

Table 1—Continued

SN	Galaxy	T	$v_{\text{hel}}$	$v_{\text{CMB}/220}$	$B_{\text{max}}$	$V_{\text{max}}$	$I_{\text{max}}$	$\Delta m_{15}$	$E(B-V)$ Gal	$E(B-V)$ max	$E(B-V)$ max35	$E(B-V)$ $V-I$	Ref.
(1)	(2)	(3)	(4)	(5)	(6)	(7)	(8)	(9)	(10)	(11)	(12)	(13)	(14)
1999gh	NGC 2986	-3	2302	2314 <sup>v</sup>	14.46	14.27	14.25	1.69	0.058	0.129	0.046	0.076	J
1999gp <sup>†</sup>	UGC 1993	3	8018	7806	16.25	16.10	16.43	0.94	0.056	0.125	0.027	-0.071	AJ
2000B	NGC 2320	-2	5944	6020	15.94	15.77	15.94	1.46	0.068	0.109	0.028	-0.030	J
2000E	NGC 6951	3	1424	1824 <sup>v</sup>	14.31	13.83	13.49	0.94	0.366	0.145	0.167	0.096	VA
2000bk	NGC 4520	0	7628	7974	16.98	16.95	16.81	1.69	0.025	0.002	0.116	0.178	KA
2000ce	UGC 4195	3	4888	4940	17.31	16.66	16.22	1.00	0.057	0.621	0.445	0.404	AJ
2000cf	MCG 11-19-25	...	10793	10805	17.15	7.10	17.31	1.27	0.032	0.034	...	-0.008	J
2000cn	UGC 11064	5	7043	6969	16.82	16.63	16.71	1.58	0.057	0.135	-0.061	0.024	J
2000dk	NGC 382	-3	5229	4932	15.63	15.56	15.74	1.57	0.070	0.002	-0.062	-0.048	J
2000fa	UGC 3770	5	6378	6533	15.99	15.95	16.12	1.00	0.069	-0.001	0.044	0.013	J
2001V	NGC 3987	3	4502	4810	14.64	14.60	14.84	0.99	0.020	0.048	0.036	0.010	ViM
2001el	NGC 1448	5	1164	1030 <sup>v</sup>	12.81	12.73	12.82	1.13	0.014	0.088	0.201	0.095	K
2002bo	NGC 3190	1	1271	1547 <sup>v</sup>	14.04	13.58	13.52	1.13	0.025	0.457	0.311	0.180	B
2002er	UGC 10743	3	2569	2804 <sup>v</sup>	14.89	14.59	14.49	1.33	0.157	0.156	0.116	0.079	Pi
(b) SNe-91T													
1991T	NGC 4527*	3	1736	(1179 <sup>V</sup> )	11.69	11.50	11.62	0.94	0.022	0.199	(0.064) <sup>2)</sup>	0.088	HA
1995ac	Anon 2245-08	1	14990	14635	17.21	17.21	17.36	0.95	0.042	-0.012	(-0.011)	0.052	RPA
1995bd	UGC 3151	5	4377	4326	17.27	16.50	...	0.88	0.498	0.305	(0.109)	...	RA
1997br	ESO 576-40	5	2085	2193 <sup>v</sup>	14.04	13.68	13.44	1.03	0.113	0.274	(0.198)	0.231	AJ
2000cx	NGC 524	-1	2379	2454 <sup>v</sup>	13.44	13.27	13.62	0.93	0.083	(0.118)	(-0.228)	-0.105	AL
(c) SNe-91bg													
1991bg	NGC 4374	-3	1060	1179 <sup>V</sup>	14.75	13.96	13.51	1.94	0.041	—	(0.005) <sup>2)</sup>	—	HA
1992K	ESO 269-G57	3	3080	3334	16.31	15.42	15.16	1.94	0.101	—	(-0.029)	—	HA
1997cn	NGC 5490	-3	4855	5092	16.93	16.39	16.14	1.90	0.027	—	...	—	J
1998bp	NGC 6495	-3	3127	3048	15.73	15.25	15.01	1.83	0.076	—	(0.059)	—	J
1998de	NGC 252	2	4990	4671	17.56	16.80	16.48	1.94	0.058	—	(0.053)	—	AJ
1999by	NGC 2841*	3	638	896 <sup>v</sup>	13.66	13.15	12.91	1.90	0.016	—	(0.011)	—	G
1999da	NGC 6411	-3	3806	3748	16.90	16.16	15.85	1.94	0.058	—	(0.027)	—	KA
1986G	NGC 5128	-1	547	317 <sup>v</sup>	12.48	11.44	...	1.69	0.115	(0.922)	(0.489)	...	A

References. — [A] Altavilla et al. (2004), [B] Benetti et al. (2004), [G] Garnavich et al. (2004), [H] Hamuy et al. (1996b,c,d), [J] Jha (2002), [K] Krisciunas et al. (2001, 2003), [L] Li et al. (2001c), [M] Mandel et al. (2001) [P] Parodi et al. (2000), [Pi] Pignata et al. (2004), [R] Riess et al. (1999), [Sa] Saha et al. (1996, 2001b), [S] Schaefer (1998), [Sl] Strolger et al. (2002), [St] Stritzinger et al. (2002), [V] Valentini et al. (2003), [Vi] Vinkó et al. (2003), [W] Wells et al. (1994).

†99aa-like SNe Ia. See § 7.1.

\*Host galaxies for which a Cepheid distance is available.

<sup>1)</sup>The SN suffers exceptionally large absorption in the host galaxy (Bottari et al. 1996); it is not used in the following.

<sup>2)</sup>The values of  $E(B-V)_{\text{max 35}}$  for SNe-91T, SNe-91bc, and for SN 2000cx and 1986G are not used in the following. They are calculated on the assumption that their intrinsic color  $(B-V)_{35}^{00}$  is given by equation (2) as for normal SNe Ia.

Table 3. Derived parameters of SNe Ia.

SN (1)	$E(B-V)_h$ (2)	$(B-V)^{00}$ (3)	$(V-I)^{00}$ (4)	$m_B^{00}$ (5)	$m_V^{00}$ (6)	$m_I^{00}$ (7)	$m_B^{\text{corr}}$ (8)	$m_V^{\text{corr}}$ (9)	$m_I^{\text{corr}}$ (10)	$(m - M)_{\text{lum}}^{00}$ (11)
(a) normal SNe Ia										
1937C	-0.022	-0.012	...	8.823	8.835	...	8.967	8.991	...	28.54
1960F	0.099	-0.034	...	11.137	11.171	...	11.284	11.308	...	30.86
1972E	-0.050	-0.006	-0.316	8.444	8.450	8.767	8.462	8.486	8.774	28.04
1972J	0.081	0.113	...	14.316	14.203	...	14.007	14.031	...	33.58
1974G	0.161	0.000	...	11.816	11.815	...	11.793	11.817	...	31.37
1980N	0.019	0.030	-0.332	12.334	12.304	12.637	12.175	12.199	12.504	31.75
1981B	0.037	0.005	...	11.832	11.827	...	11.794	11.818	...	31.37
1981D	0.193	-0.024	...	11.801	11.825	...	11.801	11.825	...	31.38
1982B	0.129	0.057	...	12.917	12.860	...	12.958	12.982	...	32.53
1983G	0.231	-0.065	...	12.018	12.083	...	11.924	11.948	...	31.50
1984A	0.190	-0.024	...	11.669	11.693	...	11.669	11.693	...	31.24
1989B	0.311	0.007	-0.162	11.075	11.068	11.223	10.925	10.949	11.105	30.50
1990N	0.034	-0.040	-0.298	12.520	12.560	12.858	12.562	12.586	12.893	32.14
1990O	-0.020	0.007	-0.385	16.281	16.274	16.659	16.357	16.381	16.704	35.93
1990T	0.019	-0.152	-0.104	16.983	17.135	17.239	17.053	17.077	17.332	36.63
1990Y	0.184	0.078	-0.403	16.985	16.907	17.307	16.897	16.921	17.210	36.47
1990af	0.007	0.028	...	17.739	17.712	...	17.404	17.428	...	36.98
1991S	0.023	-0.019	-0.304	17.590	17.609	17.912	17.647	17.671	17.952	37.22
1991U	0.062	-0.064	-0.172	16.191	16.255	16.425	16.212	16.236	16.454	35.79
1991ag	0.013	0.035	-0.367	14.369	14.334	14.701	14.469	14.493	14.753	34.04
1992A	-0.025	0.017	-0.241	12.576	12.559	12.801	12.321	12.345	12.605	31.90
1992J	0.027	0.036	-0.230	17.547	17.511	17.741	17.145	17.169	17.432	36.72
1992P	0.001	-0.042	-0.268	16.052	16.093	16.361	16.094	16.118	16.398	35.67
1992ae	0.056	-0.012	...	18.268	18.280	...	18.138	18.162	...	37.71
1992ag	0.170	-0.097	-0.380	15.623	15.719	16.096	15.612	15.636	16.112	(35.19)
1992al	-0.040	-0.054	-0.271	14.598	14.651	14.923	14.624	14.648	14.952	34.20
1992aq	0.028	-0.010	-0.143	19.267	19.277	19.420	18.896	18.920	19.150	38.47
1992au	-0.045	0.068	-0.343	18.265	18.197	18.540	17.840	17.864	18.205	37.41
1992bc	-0.081	-0.061	-0.231	15.337	15.398	15.630	15.485	15.509	15.748	35.06
1992bg	-0.030	-0.065	-0.221	16.742	16.807	17.028	16.740	16.764	17.040	36.31
1992bh	0.060	-0.032	-0.228	17.369	17.402	17.629	17.357	17.381	17.623	36.93
1992bk	-0.016	-0.069	-0.068	18.068	18.137	18.205	17.750	17.774	17.992	37.32
1992bl	-0.032	-0.009	-0.192	17.411	17.420	17.613	17.119	17.143	17.399	36.69
1992bo	-0.007	0.000	-0.136	15.774	15.774	15.911	15.396	15.420	15.632	34.97
1992bp	-0.023	-0.046	-0.210	18.330	18.377	18.587	18.089	18.113	18.421	37.66
1992br	0.010	0.034	...	19.196	19.162	...	18.795	18.819	...	38.37
1992bs	0.014	-0.025	...	18.234	18.259	...	18.204	18.228	...	37.78
1993B	0.054	-0.073	-0.234	18.188	18.261	18.494	18.099	18.123	18.447	37.67
1993H	0.122	0.088	-0.119	16.299	16.211	16.327	15.860	15.884	15.976	35.43
1993L	0.193	-0.027	...	12.640	12.666	...	12.415	12.439	...	31.99
1993O	-0.031	-0.092	-0.158	17.685	17.777	17.936	17.635	17.659	17.922	37.21
1993ac	0.040	-0.033	-0.135	17.606	17.639	17.773	17.520	17.544	17.714	37.09
1993ae	-0.057	-0.081	-0.105	15.471	15.552	15.658	15.284	15.308	15.543	34.86
1993ag	0.044	0.024	-0.303	17.682	17.657	17.960	17.526	17.550	17.832	37.10

Table 3—Continued

SN	$E(B-V)_h$	$(B-V)^{00}$	$(V-I)^{00}$	$m_B^{00}$	$m_V^{00}$	$m_I^{00}$	$m_B^{\text{corr}}$	$m_V^{\text{corr}}$	$m_I^{\text{corr}}$	$(m - M)_{\text{lum}}^{00}$
(1)	(2)	(3)	(4)	(5)	(6)	(7)	(8)	(9)	(10)	(11)
1993ah	-0.023	-0.037	-0.286	16.322	16.359	16.645	16.117	16.141	16.502	35.69
1994D	-0.040	-0.062	-0.146	11.916	11.978	12.124	11.814	11.838	12.064	31.39
1994M	0.056	-0.029	-0.204	16.050	16.079	16.282	15.839	15.863	16.133	35.41
1994Q	0.035	0.028	-0.338	16.243	16.215	16.552	16.329	16.353	16.597	35.90
1994S	-0.042	-0.019	-0.281	14.858	14.877	15.159	14.904	14.928	15.190	34.48
1994T	0.047	0.044	-0.250	17.058	17.014	17.264	16.797	16.821	17.054	36.37
1994ae	0.033	-0.013	-0.382	12.907	12.920	13.302	13.040	13.064	13.393	32.61
1995D	-0.009	-0.009	-0.364	13.234	13.243	13.607	13.267	13.291	13.626	32.84
1995E	0.647	0.046	...	14.347	14.301	...	14.244	14.268	...	33.82
1995ak	0.055	-0.103	-0.232	15.734	15.837	16.068	15.574	15.598	15.979	35.15
1995al	0.071	0.025	-0.362	13.043	13.018	13.379	13.138	13.162	13.431	32.71
1996C	0.026	-0.009	-0.262	16.440	16.450	16.711	16.528	16.552	16.769	36.10
1996X	-0.015	-0.004	-0.250	13.032	13.036	13.286	12.883	12.907	13.173	32.46
1996Z	0.332	-0.036	...	13.135	13.172	...	13.070	13.094	...	32.64
1996ab	0.101	-0.013	...	19.040	19.053	...	19.173	19.197	...	38.75
1996ai	1.611	0.075	...	11.023	10.948	...	11.107	11.131	...	(30.68)
1996bk	0.308	0.104	...	13.641	13.538	...	13.192	13.216	...	32.77
1996bl	0.042	-0.034	-0.225	16.550	16.584	16.808	16.551	16.575	16.812	36.13
1996bo	0.257	0.036	...	14.898	14.862	...	14.734	14.758	...	34.31
1996bv	0.117	0.008	-0.311	14.913	14.905	15.213	15.050	15.074	15.301	34.62
1997E	0.024	-0.008	-0.202	14.996	15.003	15.205	14.807	14.831	15.064	34.38
1997Y	0.035	-0.072	-0.128	15.084	15.156	15.283	15.025	15.049	15.256	34.60
1997bp	0.169	-0.013	-0.451	13.322	13.335	13.782	13.394	13.418	13.831	32.97
1997bq	0.159	0.117	-0.341	13.890	13.774	14.112	13.848	13.872	14.035	33.42
1997cw	0.334	0.073	-0.346	14.481	14.408	14.748	14.463	14.487	14.703	(34.04)
1997dg	0.057	-0.045	-0.207	16.670	16.716	16.922	16.667	16.691	16.927	36.24
1997do	0.055	-0.018	-0.284	14.103	14.120	14.403	14.166	14.190	14.446	33.74
1997dt	0.496	0.007	-0.189	13.595	13.588	13.768	13.611	13.635	13.768	33.19
1998V	0.016	-0.042	-0.186	15.019	15.060	15.246	15.055	15.079	15.278	34.63
1998ab	0.079	-0.086	-0.177	15.581	15.667	15.842	15.759	15.783	15.990	(35.33)
1998aq	-0.052	-0.022	...	12.353	12.375	...	12.339	12.363	...	31.91
1998bu	0.279	0.056	-0.191	11.098	11.043	11.228	11.013	11.037	11.140	30.59
1998dh	0.120	0.072	-0.307	13.522	13.451	13.755	13.377	13.401	13.619	32.95
1998dk	0.130	0.016	-0.299	14.275	14.259	14.555	14.278	14.302	14.544	33.85
1998dm	0.239	-0.063	-0.173	13.646	13.710	13.878	13.692	13.716	13.923	33.27
1998dx	-0.026	-0.045	-0.139	17.638	17.683	17.822	17.377	17.401	17.641	36.95
1998ec	0.131	0.014	-0.293	15.614	15.600	15.890	15.600	15.624	15.868	35.17
1998ef	0.021	-0.064	-0.223	14.833	14.897	15.120	14.941	14.965	15.210	34.52
1998eg	0.043	-0.046	-0.206	15.959	16.005	16.211	15.944	15.968	16.207	35.52
1998es	0.055	0.033	-0.354	13.660	13.626	13.979	13.761	13.785	14.032	(33.34)
1999X	0.139	-0.011	-0.245	15.812	15.823	16.065	15.797	15.821	16.050	35.37
1999aa	-0.022	0.022	-0.382	14.838	14.815	15.198	14.959	14.983	15.270	(34.53)
1999ac	0.077	-0.063	-0.202	13.869	13.932	14.133	13.957	13.981	14.209	(33.53)
1999aw	-0.045	0.033	-0.382	16.893	16.860	17.243	17.031	17.055	17.323	36.61
1999cc	-0.002	0.009	-0.237	16.763	16.754	16.991	16.520	16.544	16.806	36.09

Table 3—Continued

SN (1)	$E(B-V)_h$ (2)	$(B-V)^{00}$ (3)	$(V-I)^{00}$ (4)	$m_B^{00}$ (5)	$m_V^{00}$ (6)	$m_I^{00}$ (7)	$m_B^{\text{corr}}$ (8)	$m_V^{\text{corr}}$ (9)	$m_I^{\text{corr}}$ (10)	$(m - M)_{\text{lum}}^{00}$ (11)
1999cl	0.918	0.264	-0.451	11.605	11.341	11.773	11.351	11.375	11.495	(30.93)
1999dk	0.024	0.012	-0.372	14.732	14.720	15.091	14.597	14.621	14.982	34.17
1999dq	0.096	-0.006	-0.350	14.078	14.084	14.432	14.200	14.224	14.514	(33.77)
1999ee	0.234	0.066	-0.385	13.992	13.927	14.307	14.040	14.064	14.312	33.61
1999ef	-0.010	0.053	-0.399	17.201	17.148	17.547	17.172	17.196	17.501	36.75
1999ej	0.015	-0.036	-0.172	15.304	15.340	15.512	15.123	15.147	15.386	(34.70)
1999ek	0.177	0.042	-0.313	15.023	14.981	15.291	14.959	14.983	15.223	34.53
1999gd	0.366	0.003	-0.197	15.515	15.513	15.702	15.472	15.496	15.662	35.05
1999gh	0.084	0.048	-0.166	13.917	13.869	14.033	13.506	13.530	13.714	33.08
1999gp	0.027	0.067	-0.438	15.922	15.855	16.293	15.957	15.981	16.288	(35.53)
2000B	0.036	0.066	-0.306	15.530	15.464	15.769	15.248	15.272	15.537	34.82
2000E	0.136	-0.022	-0.315	12.313	12.335	12.648	12.410	12.434	12.716	31.98
2000bk	0.099	-0.094	-0.023	16.518	16.611	16.632	16.205	16.229	16.430	35.78
2000ce	0.490	0.103	-0.281	15.287	15.184	15.456	15.261	15.285	15.395	34.84
2000cf	0.013	0.005	-0.269	16.971	16.966	17.235	16.847	16.871	17.136	36.42
2000cn	0.033	0.100	-0.197	16.467	16.366	16.563	16.087	16.111	16.250	35.66
2000dk	-0.036	0.036	-0.224	15.473	15.438	15.662	15.144	15.168	15.406	34.72
2000fa	0.018	-0.047	-0.284	15.640	15.687	15.971	15.717	15.741	16.034	35.29
2001V	0.032	-0.012	-0.308	14.443	14.454	14.761	14.502	14.526	14.799	34.08
2001el	0.128	-0.062	-0.277	12.285	12.347	12.622	12.293	12.317	12.640	31.87
2002bo	0.316	0.119	-0.390	12.783	12.665	13.048	12.666	12.690	12.917	32.24
2002er	0.117	0.026	-0.259	13.819	13.793	14.049	13.644	13.668	13.907	33.22
(b) SNe Ia-T										
1991T	0.143	0.025	-0.338	11.077	11.052	11.387	11.141	11.165	11.417	
1995ac	0.020	-0.062	-0.231	16.965	17.027	17.257	17.083	17.107	17.355	
1995bd	0.305	-0.033	...	14.113	14.147	...	14.255	14.279	...	
1997br	0.252	-0.005	-0.240	12.656	12.661	12.896	12.686	12.710	12.911	
2000cx	0.007	see Table 6								
(c) SNe Ia-bg										
1991bg	0.00 <sup>1)</sup>	0.749	0.397	14.582	13.833	13.436				
1992K	0.00 <sup>1)</sup>	0.789	0.129	15.896	15.107	14.978				
1997cn	0.00 <sup>1)</sup>	0.513	0.215	16.819	16.306	16.091				
1998bp	0.00 <sup>1)</sup>	0.404	0.141	15.418	15.014	14.873				
1998de	0.00 <sup>1)</sup>	0.702	0.245	17.322	16.620	16.376				
1999by	0.00 <sup>1)</sup>	0.494	0.219	13.594	13.100	12.881				
1999da	0.00 <sup>1)</sup>	0.682	0.235	16.662	15.980	15.746				
1986G	see Table 7									

<sup>1)</sup> $E(B-V)_{\text{host}}$  assumed to be 0.00 (see § 7.2).

Note. — Negative extinction and absorption corrections in the host galaxies have been subtracted algebraically in columns 3-9 in order not to skew the distribution function and not to shift the *mean* value. For the most probable values of *individual* SNe Ia negative extinctions  $E(B-V)_{\text{host}}$  and corresponding absorption corrections should be set to zero.